Lawrence Berkeley National Laboratory
Recent Work

Title

DETERMINATION OF DIPOLE COUPLING CONSTANTS USING HETERONUCLEAR MULTIPLE QUANTUM NMR

Permalink

https://escholarship.org/uc/item/5gz368t4

Authors

Weitekamp, D.P.
Garbow, J.R.
Pines, A.

Publication Date

1982-03-01

eScholarship.org Powered by the California Digital Library
University of California

LBL-14206
Preprint

Lawrence Berkeley Laboratory

UNIVERSITY OF CALIFORNIA

RECEIVED
LAWRENCE
BERKELEY LABORATORY
MAY 7 1982
LIBRARY AND
DOCUMENTS SECTION

Materials & Molecular Research Division

Submitted to the Journal of Chemical Physics

DETERMINATION OF DIPOLE COUPLING CONSTANTS USING HETERONUCLEAR MULTIPLE QUANTUM NMR

D.P. Weitekamp, J.R. Garbow and A. Pines

March 1982

TWO-WEEK LOAN COPY

This is a Library Circulating Copy which may be borrowed for two weeks. For a personal retention copy, call Tech. Info. Division, Ext. 6782.

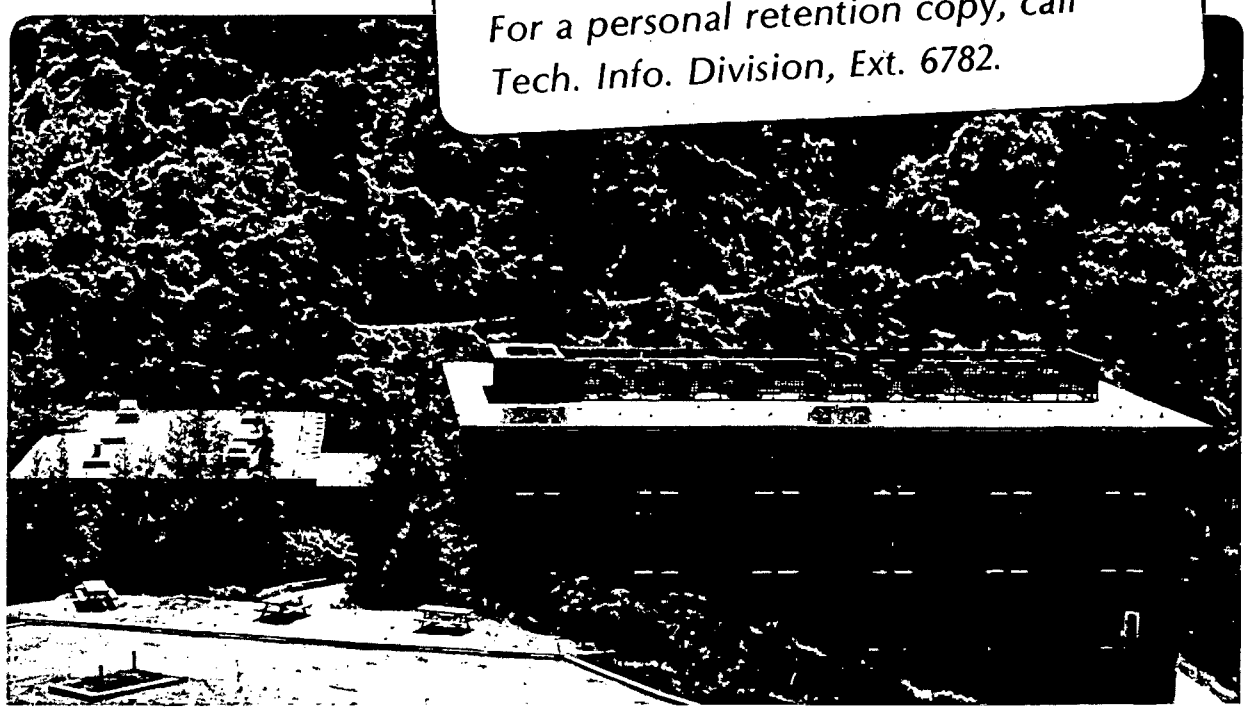

Prepared for the U.S. Department of Energy under Contract DE-AC03-76SF00098

LBL-14206

DISCLAIMER

This document was prepared as an account of work sponsored by the United States Government. While this document is believed to contain correct information, neither the United States Government nor any agency thereof, nor the Regents of the University of California, nor any of their employees, makes any warranty, express or implied, or assumes any legal responsibility for the accuracy, completeness, or usefulness of any information, apparatus, product, or process disclosed, or represents that its use would not infringe privately owned rights. Reference herein to any specific commercial product, process, or service by its trade name, trademark, manufacturer, or otherwise, does not necessarily constitute or imply its endorsement, recommendation, or favoring by the United States Government or any agency thereof, or the Regents of the University of California. The views and opinions of authors expressed herein do not necessarily state or reflect those of the United States Government or any agency thereof or the Regents of the University of California.

DETERMINATION OF DIPOLE COUPLING CONSTANTS USING HETERONUCLEAR MULTIPLE QUANTUM NMR

D. P. Weitekamp, J. R. Garbow and A. Pines

Department of Chemistry and

Lawrence Berkeley Laboratory

University of California, Berkeley CA 94720

This work was supported by the Director, Office of Energy Research, Office of Basic Energy Sciences, Materials Sciences Division of the U.S. Department of Energy under Contract Number DE-AC03 -76SF00098.

ABSTRACT

The problem of extracting dipole couplings from a system of N spins I = 1/2 and one spin S by NMR techniques is analyzed. The resolution attainable using a variety of single quantum methods is reviewed. The theory of Heteronuclear Multiple Quantum (HMQ) NMR is developed, with particular emphasis being placed on the superior resolution available in HMQ spectra. Several novel pulse sequences are introduced, including a two-step method for the excitation of HMQ coherence. Experiments on partially oriented [1 - ^{13}C] benzene demonstrate the excitation of the necessary HMQ coherence and illustrate the calculation of relative line intensities. Spectra of high order HMQ coherence under several different effective Hamiltonians achievable by multiple pulse sequences are discussed. A new effective Hamiltonian, scalar heteronuclear recoupled interactions by multiple pulse (SHRIMP), achieved by the simultaneous irradiation of both spin species with the same multiple pulse sequence, is introduced. Experiments are described which allow heteronuclear couplings to be correlated with an S-spin spreading parameter in spectra free of inhomogeneous broadening.

I. Introduction

A. Dilute heteronuclear systems

The measurement of direct dipolar coupling constants between nuclear spins in solids and in liquid crystal phases has proven to be an uniquely sensitive probe of molecular shape and ordering in these anisotropic phases. In liquid crystals [1], where diffusion effectively averages away the couplings between molecules, the spin system is intramolecular. For a typical organic molecule this system consists of a number of protons ($N \tilde{=} 10$) and perhaps a nitrogen nucleus or a ^{13}C nucleus randomly distributed at natural abundance of 1% among the carbon sites. This same sort of intramolecular spin system might be created in other anisotropic phases by dilution of a protonated species into a deuterated host, by isolation of molecules in a low temperature matrix, or by adsorption on a surface.

B. Physical picture of single quantum and multiple quantum methods

Accurate determination of heteronuclear dipolar couplings by NMR is dependent upon the ability to obtain spectra which are well-resolved and highly sensitive to these particular spin interactions. Previous attempts to achieve these goals have focused on the use of multiple pulse sequences to decouple homonuclear dipolar couplings between abundant spins. Fig. 1(a) is a schematic illustration of the resulting situation. The proton spins independently experience the local field of the ^{13}C

nucleus and vice versa. Couplings between protons are assumed to be effectively absent, thus simplifying analysis considerably.

Even with this idealized removal of homonuclear interactions, the spectrum of the S spin consists of 2^N transition frequencies, corresponding to the different ways of arranging the proton spins up or down, only one of which is depicted in the figure. Furthermore, the sign of the heteronuclear couplings is absent from the single quantum local field spectrum of either spin species.

These difficulties are overcome by the use of heteronuclear multiple quantum (HMQ) NMR. The proton spins are excited as a coherent group, as suggested by Fig. 1(b), where one of the N possible groupings of N-1 protons is depicted. This grouping leads to an ordered field interaction between the protons and the heteronuclear spin in which sums of the local fields are measured, thereby providing information on relative signs. The relatively few distinct ways in which a large number of the abundant spins can be grouped restricts the number of transitions and increases resolution. This work demonstrates and discusses a number of experimental approaches to the excitation of HMQ coherence and its use as a high resolution time domain probe for heteronuclear couplings. Particular attention is given to comparison of the resolution and information content of these and alternative single quantum methods.

C. Hamiltonian description

Nuclear magnetic resonance of a spin system of N spins I and one spin S can in principle yield dipolar couplings and the corresponding geometric information in a much simpler and more reliable manner than that of the homonuclear spin system alone. There are several recognized reasons why the apparent complication of introducing a heteronuclear spin can in fact be simplifying. These are best discussed in the doubly rotating frame, the interaction representation which removes the time dependence of r.f. irradiation at the Larmor frequencies of both spin species. The spin Hamiltonian is:

$$\mathcal{H} = \mathcal{H}_I^Z + \mathcal{H}_S^Z + \mathcal{H}_{II}^D + \mathcal{H}_{II}^J + \mathcal{H}_{IS} + \mathcal{H}_S^Q \quad . \qquad (1)$$

The first two terms are the Zeeman interactions of the spins with the magnetic field, which in this interaction frame consist of the offsets of individual nucleus resonance frequencies from the spectrometer references:

$$\mathcal{H}_I^Z = - \sum_{i=1}^{N} \nu_i I_{Zi} - (\nu(\underset{\sim}{r}) + \Delta\nu_I) I_Z \qquad (2a)$$

$$\mathcal{H}_S^Z = - \nu_S S_Z - [(\gamma_S/\gamma_I)\ \nu(\underset{\sim}{r}) + \Delta\nu_S]\ S_Z \quad . \qquad (2b)$$

Eq.(2) embodies the conventions that $\sum_i \nu_i = 0$ and $\int \nu(\underset{\sim}{r}) d\underset{\sim}{r} = 0$. It is assumed that any fields which vary with position $\underset{\sim}{r}$ in the sample are constant over molecular dimensions. The third term in Eq. (1) is the dipolar interaction among the I spins,

$$\mathcal{H}_{II}^{D} = \sum_{i<j} D_{ij} \, (3I_{Zi}I_{Zj} - \underset{\sim}{I}_i \cdot \underset{\sim}{I}_j) \quad , \tag{3}$$

while the fourth describes the much smaller indirect interactions among these spins,

$$\mathcal{H}_{II}^{J} = - \sum_{i<j} J_{ij} \, \underset{\sim}{I}_i \cdot \underset{\sim}{I}_j \quad . \tag{4}$$

The fifth term accounts for both the direct and indirect heteronuclear couplings,

$$\mathcal{H}_{IS} = - \sum_{i} 2F_{iS} I_{Zi} S_Z \quad , \tag{5}$$

where $F_{iS} = \frac{1}{2}(J_{iS} + 2D_{iS})$. A quadrupole term is included for the case $S \geq 1$. This has the form

$$\mathcal{H}_{S}^{Q} = (\nu_Q/3)(3S_Z^2 - S(S+1)) \quad . \tag{6}$$

The I spins will always be assumed to be spin 1/2 nuclei.

The indirect scalar couplings between spins A and B, J_{AB}, are usually approximated by their liquid state values and the Zeeman parameters are often not readily interpreted in terms of molecular geometry. It is the dipolar constants between spins A and B, D_{AB}, which are the principal unknowns of interest. These dipolar coupling constants are purely geometric quantities:

$$D_{AB} = - \left(\frac{h\gamma_A\gamma_B}{4\pi^2} \right) < P_2(\cos\theta_{AB})/r_{AB}^3 > \quad . \tag{7}$$

D. Advantages of heteronuclear systems for determination of molecular geometry

The first possible advantage of the heteronuclear system over the purely homonuclear case is that the number of heteronuclear couplings is N, in contrast to the N(N-1)/2 homonuclear couplings. While this represents less information, it also means that if a spectrum determined only by heteronuclear unknowns can be obtained, then spectral simulation is greatly simplified. If the S spin can take a variety of positions in the molecule, as with ^{13}C, then the information is abundant in any case.

Secondly, investigation of $\mathcal{H}_{IS}$ with $\mathcal{H}_{II}^{D}$ removed by multiple pulse techniques improves the validity of the approximation of neglecting intermolecular spin interactions in solids. This is because the large gyromagnetic ratio of typical I spins (^{1}H, ^{19}F) and their position on the outside of molecules lead to significant intermolecular terms in $\mathcal{H}_{II}^{D}$ at dilutions where such terms in $\mathcal{H}_{IS}$ are negligible.

Thirdly, the individual terms in the heteronuclear coupling Hamiltonian commute with one another and thus the spectrum of $\mathcal{H}_{IS}$ alone is particularly simple.[2] The number of transitions is smaller and the relationships between transition frequencies and couplings are simpler than for a sum of noncommuting terms such as appears for the homonuclear case or the full Hamiltonian of Eq. (1).

Finally, the heteronuclear spin (eg. ^{13}C, ^{15}N, ^{31}P, ^{2}H, ^{14}N)

will often have a large chemical shift range or quadrupolar splitting, which can serve as a spreading parameter. This allows an association to be made, for example by two dimensional spectroscopy, between the observed dipolar splittings and the spreading parameter which is assignable to a specific site.

E. Outline

These realizations were the motivation for the technique of ^{13}C local field spectroscopy.[2-10] In section II the resolution of this and other single quantum methods is reviewed. The techniques of S spin single quantum local field spectroscopy, as well as the less familiar I spin analog, are considered with particular attention given to their resolution limitations.

Section III summarizes previous work on HMQ NMR and develops theoretically its advantages for the determination of the heteronuclear dipolar couplings in anisotropic systems.

Section IV experimentally demonstrates certain aspects of the method including a novel two-step method of excitation of the HMQ coherence. The high quantum spectra of partially enriched [1-^{13}C] benzene serve as examples.

In Section V the concept of scalar heteronuclear recoupled interactions by multiple pulse (SHRIMP) is introduced and the proposed use of this new coherent averaging technique during the HMQ evolution period is outlined.

Section VI discusses how the HMQ spectra arising from different molecular species may be separated from one another by introducing the S spin chemical shift or quadrupole coupling into the evolution period.

II. Spectral Resolution of the Single Quantum Methods

A. The number of transitions

A convenient a priori estimate of achievable spectral resolution is obtained by enumerating the transitions allowed with a certain technique. Ideally, this number is sufficiently small that individual transitions can be resolved. Roughly, this requires that

$$Z < M_2^{1/2} T_2 \tag{8}$$

where Z is the number of allowed transitions, $M_2^{1/2}$ is the square root of the second moment of the spectrum and T_2 is the relaxation time determining the width of individual transitions. For many anisotropic systems this irreversible relaxation sets an upper limit of $Z = 10^2 - 10^3$.

The increase in spectral complexity which comes with an increase in the number of proton spins is illustrated graphically in Fig. 2(a). Here the logarithm of the number of spectral lines as a function of the number of protons (N) is plotted for the normal single quantum ^{13}C and single quantum ^{1}H spectra for molecules containing one ^{13}C nucleus and N protons. The number of spectral lines grows exponentially with increasing number of protons, quickly resulting in spectra with far too many lines to allow extraction of useful coupling information. As an illustration of this, Figure 3(a) shows a simulation of the single quantum ^{13}C

spectrum of [1 - ^{13}C] benzene partially oriented in a liquid crystal solvent.

B. S spin local field spectroscopy

In the last few years several groups have addressed the problem of extracting heteronuclear dipolar coupling constants in solids [3-7] and in liquid crystals[8] with the technique of ^{13}C local field spectroscopy. Recently this technique has been applied to powder samples rotating at the magic angle.[9,10] Recognizing that couplings among protons were responsible for much of the ^{13}C spectral complexity, they employed proton multiple pulse sequences[11-13] or magic angle irradiation[14] to eliminate proton homonuclear dipolar couplings. In addition, they sorted out spectra due to inequivalent ^{13}C's by collecting proton decoupled carbon spectra in a second time dimension. Double Fourier transformation then yielded ^{13}C spectra recorded in the absence of proton-proton dipole couplings and separated out by their ^{13}C chemical shifts.

Figure 3(b) is a simulation of an ideal single quantum ^{13}C local field spectrum of partially oriented [1 - ^{13}C] benzene. Even in this simple system the tendency of the transitions to cluster into unresolvable multiplets is apparent. Within the two well-resolved groups of lines, the line density is similar to the unperturbed ^{13}C spectrum of Fig. 3(a). The number of transitions depends exponentially on the number of coupled protons, whether or not the protons are coupled to one another

(Fig. 2). As a result, often only the largest proton-carbon coupling is resolved. The smaller couplings appear only as a line broadening, which is difficult to analyze quantitatively. The interpretation is further confounded by the insensitivity of the spectrum to the sign of the couplings.

C. I spin local field spectroscopy

An alternate version of the single quantum local field experiment is to observe the effects of $\mathcal{H}_{IS}$ on the abundant I spin spectrum with $\mathcal{H}_{II}^{D}$ again eliminated by a multiple pulse sequence. Studies of this type have been made on protons in powder solid state samples.[15,16] Here we consider the resolution potential of such spectra when orientational inhomogeneity broadening is absent, as in single crystals or liquid crystals.

In the limit that $\mathcal{H}_{II} = 0$ the ^{1}H local field spectrum consists of just N pairs of lines. This dependence of the number of lines on N is indicated in the lowest curve of Fig. 2(b). Each pair is the spectrum of a single proton, and the splittings $2K|F_{iS}|$ give the parameters of $\mathcal{H}_{IS}$ directly once the multiple pulse scale factor K is established. The resolution advantage over the ^{13}C local field spectrum is considerable since the same information which was present in 2^{N} lines is now present in only 2N lines.

Although, in the limit that $\mathcal{H}_{II} = 0$, these experiments would provide information on $\mathcal{H}_{IS}$ with a minimum number of transitions, they can provide no information on the sign of the F_{iS} parameters. Furthermore, this limit is never actually reached, since the indirect terms $\mathcal{H}_{II}^{J}$ are not removed by multiple pulse

sequences. This is illustrated in Figure 4(a) which shows the simulated single quantum proton spectrum of oriented [1 - ^{13}C] benzene in the absence of homonuclear dipolar couplings. (The spectrum with all couplings present has been previously reported.[17]) Although the largest indirect proton-proton coupling is less than 10 Hz, the spectrum consists of multiplets of densely packed transitions, each multiplet spanning a width of several times this value. Figure 4(b) illustrates the spectrum of this same molecule in the hypothetical absence of any ^{1}H - ^{1}H couplings. Comparison of these two spectra indicates that the indirect proton couplings set a limit on the accuracy with which F_{iS} can be measured by single quantum local field spectroscopy. Nevertheless, comparison of Fig. 4(a) and Fig. 3(b) does demonstrate the potential resolution advantage of I spin single quantum local field spectra over the S spin version with respect to measuring the magnitude of small heteronuclear couplings.

III. Heteronuclear Multiple Quantum NMR

A. Background

The principle focus of HMQ NMR experiments to date has been the observation of dilute S spin transitions with the greater sensitivity afforded by the abundance and larger gyromagnetic ratio of the I spins. In solids the multiple quantum transitions of the S = 1 spins of deuterium [18,19] and ^{14}N[20,21] and the S = 3/2 spin of ^{23}Na[22] have been observed with the aid of cross polarization to protons. In these solid state samples the spin

system is of macroscopic dimension and the coherence transfer is treated with the spin temperature formalism.

In liquids, I_nS spin 1/2 systems have been used to demonstrate such fundamental multiple quantum phenomena as the relaxation of forbidden and degenerate coherences[23-25], heteronuclear coherence transfer echoes [26] and the indirect detection of dilute spin chemical shifts independent of γ_S.[27] Recently, the ^{14}N double quantum spectrum of ammonium ion in aqueous solution has been detected using only ^{14}N magnetization[28] and only ^{1}H magnetization.[29]

In liquid crystals, the deuterium double quantum transition of the I_2S system of partially oriented CH_2DCN has been detected through the proton transverse magnetization using a pulsed coherence transfer, as well as other preparation and detection schemes.[30]

B. Formalism

The Hamiltonian describing the heteronuclear couplings was given in Eq. (5) and contains no flip-flop terms, since these do not conserve Zeeman energy. Consequently the total Zeeman quantum numbers for each species separately are good quantum numbers for the free evolution of the system. It is therefore useful to characterize elements of the density operator describing the system by the quantities n^I and n^S defined such that

$$\rho(\tau) = \sum_{n^I} \sum_{n^S} \rho_{n^I,n^S}(\tau) \qquad (9)$$

$$[I_Z, \rho_{n^I, n^S}] = n^I \rho_{n^I, n^S} \tag{10}$$

$$[S_Z, \rho_{n^I, n^S}] \quad n^S \rho_{n^I, n^S} \quad . \tag{11}$$

The quantities n^I and n^S are differences in Zeeman quantum numbers between the states described by ρ. Thus $n^I_{ij} = m^I_i - m^I_j$ and $n^S_{ij} = m^S_i - m^S_j$ for particular states $|i\rangle$ and $|j\rangle$. The defining commutation relations of Eqs. (10) and (11) insure that each set of indices (n^I, n^S) represents a separate spectrum which may be isolated through its characteristic modulation properties under phase shifts of the irradiation frequencies[31-33] or by its dephasing and rephasing properties under field gradients.[26,29,34,35] A generalized diagram of the HMQ experiment is given in Fig. 5. HMQ coherences are prepared by the propagator U and evolve under the action of the effective Hamiltonian $\mathcal{H}_1$ during the time period t_1. The propagator V mixes these coherences into observable single quantum operators which are sampled during time period t_2. The preparation and mixing periods are collectively referred to as excitation periods.

While the initial magnetization and the detected magnetization can be that of either the I or S spins, the signal-to-noise advantage[27,30] of using only the magnetization of the spin with greater gyromagnetic ratio is considerable. In most cases of interest, the I spins are protons and only their magnetization need be considered. As discussed in Section VI this is not inconsistent

with making use of the S spin spreading parameters.

For S = 1/2, a convenient operator basis for describing the dynamics of the combined I-S coherence are the simple products, one factor for each spin, of the single spin operators:

$$S_+ = |\alpha><\beta| \quad S_- = |\beta><\alpha| \quad S_0^+ = |\alpha><\alpha| \quad S_0^- = |\beta><\beta|. \quad (12)$$

An analogous definition holds for the individual I spin operators: I_{+i}, I_{-i}, I_{0i}^+ and I_{0i}^- where the nuclear index runs from 1 to N. Any product of one such operator for each spin may be classified with respect to the quantum number n^I by adding up the subscripts of the I spin factors, and the quantum number n^S which is the subscript of the S-spin factor. The usefulness of this operator basis is that any of its members is an eigenoperator for evolution under $\mathcal{H}_{IS}$ and that it includes the relevant part of the prepared density operator for several of the experiments discussed.

C. The higher order HMQ spectra

The HMQ spectra characterized by n^I = N, N - 1 and n^S = 0, ±1 are of particular interest since they have the fewest transitions compatible with full determination of the heteronuclear couplings F_{iS}. Each of these spectra will be discussed for S = 1/2 with regard to the number of transitions and to the transition frequencies in the limit that $\mathcal{H}_{II}$ = 0. The transition frequencies are approximate, since $\mathcal{H}_{II}^J$ is neglected. The important point is that the number of transitions does not drastically increase when $\mathcal{H}_{II}^J$ is admitted, unlike the situation for

single quantum local field spectroscopy of the I spins. Thus numerical inclusion of $\mathcal{H}_{II}^{J}$, the parameters of which may be closely approximated by the liquid state values, does not seriously affect the resolution and perturbs the frequencies only slightly from the analytical forms given below.

The experimental removal of $\mathcal{H}_{II}^{D}$ by multiple pulse sequences results in a scaling of the terms $\mathcal{H}_{I}^{Z}$ and $\mathcal{H}_{IS}$ by a common factor K[11-13]. Because the discussion is simplified when n^I is a good quantum number, it will be assumed in this section that the effective Hamiltonian $\mathcal{H}_1$ during the evolution period is

$$\mathcal{H}_1 = \overline{\mathcal{H}_{IS}^{(0)}} + \mathcal{H}_{II}^{J} = K \sum_i 2F_{iS} I_{Zi} S_Z + \sum_{i<j} J_{ij} \underset{\sim}{I}_i \cdot \underset{\sim}{I}_j \quad (13)$$

This effective heteronuclear coupling is obtained, for example, by the HW - 8 cycle[11,13] where K = 1/3. Such a pulse sequence may be augmented by simultaneous π pulses to both the I and S spins in between cycles in order to remove the Zeeman terms, and hence the magnet inhomogeneity, from the evolution period. Other pulse sequences resulting in the $\mathcal{H}_1$ of Eq. (13) are possible.[36]

1. $n^I = N$, $n^S = 1$

Consider first the evolution during t_1 of the total spin coherence of the combined I-S system. This coherence is characterized by quantum numbers $n^I = N$, $n^S = 1$ and the eigenoperator is $S_+ \prod_i I_{+i}$, which commutes with $\mathcal{H}_{IS}$. In fact, this coherence also commutes with the homonuclear spin-spin couplings so that its evolution under the full Hamiltonian of Eq. (1) is

determined only by the sum of the Zeeman terms.

2. $n^I = N,\ n^S = 0$

The simplest case which can yield dipolar coupling information is that of the two eigenoperators with $n^I = N,\ n^S = 0$. These are $S_0^{\pm} \prod_i I_{+i}$ and their commutators with $\overline{\mathcal{H}}_{IS}^{(0)}$ are given by

$$[\overline{\mathcal{H}_{IS}^{(0)}},\ S_0^{\pm} \prod_{i=1}^{N} I_{+i}] = \mp K(\sum_i F_{iS}) S_0^{\pm} \prod_{i=1}^{N} I_{+i} \quad . \qquad (14)$$

Since the $n^I = N,\ n^S = 0$ operators commute with the I-I couplings they are the correct eigenoperators whether or not $\mathcal{H}_{II}$ has been removed. This commutator shows that the spectrum $n^I = N,\ n^S = 0$ consists of a pair of lines with splitting $2K|\sum_i F_{iS}|$ if a multiple pulse sequence is used and $2|\sum_i F_{iS}|$ if only a single π pulse to both the I and S spins at $t_1/2$ is applied. A comparison of these two spectra provides an experimental measurement of K which is free of inhomogeneous broadening.

3. $n^I = N - 1,\ n^S = 1$

The 2N operators characterized by $n^I = N - 1,\ n^S = 1$ are eigenoperators under $\overline{\mathcal{H}}_{IS}^{(0)}$ and their eigenvalues are determined by the commutators

$$[\overline{\mathcal{H}_{IS}^{(0)}},\ S^+ I_{0i}^{\pm} \prod_{j \neq i} I_{+j}] = \pm K F_{iS} (S^+ I_{0i}^{\pm} \prod_{j \neq i} I_{+j}) \quad . \qquad (15)$$

This corresponds to a spectrum of N pairs of lines, each pair giving the magnitude of one of the heteronuclear couplings F_{iS}.

No information regarding the relative signs of these couplings is supplied. These transitions yield the same information as S single quantum local field experiments (Section (IIB)), but the information is now present in 2N lines instead of 2^N lines. In contrast to the I single quantum local field experiment (Section (IIC)) the presence of homonuclear I-I couplings does not increase the number of lines in the $n^I = N - 1$, $n^S = 1$ spectrum. Experiments done without removal of homonuclear dipole couplings (or those in which dipole couplings are removed, but indirect spin-spin couplings are not negligible) do not suffer a loss in resolution as do the corresponding single quantum local field experiments.

4. $n^I = N - 1$, $n^S = 0$

Finally we consider the case where $n^I = N - 1$, $n^S = 0$. There are 4N eigenoperators of $\bar{\mathcal{H}}_{IS}^{(0)}$ having eigenvalues determined by the commutators

$$[\overline{\mathcal{H}_{IS}^{(0)}} \ , \ S_0^{\pm} \ I_{0i}^{\pm} \prod_{j\neq i} I_{+j}] = \mp K(\sum_{j\neq i} F_{jS})(S_0^{\pm} \ I_{0i}^{\pm} \prod_{j=i} I_{+j}) \qquad (16)$$

where the sign on the right is defined with respect to the superscript of the S-spin operator. Each eigenvalue is two-fold degenerate. The resulting spectrum consists of N pairs of lines, with splittings proportional to the sum of all but one of the I-S couplings. The one coupling absent is different for each of the N pairs, so there are N linearly independent equations whose solutions give the N F_{iS} couplings, including relative signs. When $\mathcal{H}_{II} \neq 0$, the degeneracy is lifted and 2N pairs of lines are possible.

This analysis could be extended to lower quantum spectra with equally simple expressions for the eigenvalues. The spectra in the limit $\mathcal{H}_{II} = 0$ will always consist of pairs of lines whose splittings are proportional to sums and differences of the heteronuclear coupling constants. Not surprisingly, the number of lines rapidly increases as n^I decreases and resolution consequently decreases. The heteronuclear Hamiltonian $\mathcal{H}_{IS}$ is, however, fully determined by the spectra discussed above.

IV. Experiments

A. Pulse sequences and spectra

The experiments were performed on [1 - ^{13}C] benzene enriched to 90% and dissolved at 40 mole % in the nematic liquid crystal p-octylphenyl 2-chloro-4-(p-heptylbenzoyloxy) benzoate (Eastman 15320). The temperature was regulated at 26.0 ±0.1°C. The home-built spectrometer, described elsewhere[37], operates at 180 MHz proton Larmor frequency. Proton signal was detected throughout with sampling of the transverse magnetization at time $t_2 = 0$ only.

Figure 6 illustrates the portions of the [1 - ^{13}C] benzene energy level diagram relevant to these experiments. A simple pulse sequence for obtaining spectra characterized by $|n^I| \leq N$, $n^S = 0$ is illustrated in Figure 7(a). The pulse sequence of Figure 7(b) employs, in addition, a pulsed magnetic field gradient in the mixing period to suppress signal from all but a single n^I value.[34] This reduces the computer memory storage requirements for the experiment. Experimental spectra obtained for $n^I = 5$ and $n^I = 6$ using this sequence are shown in Figure 8(a). The $n^I = 6$

spectrum shows a doublet whose splitting measures $2\sum_i F_{iS}$ independent of I-I couplings. The central peak in this spectrum is the total spin transition from the unlabeled molecules. The $n^I = 5$ spectrum consists of one pair of lines due to unlabeled molecules and three pairs from [1 - ^{13}C] benzene molecules. The energy level diagram suggests that there should be eight pairs of $n^I = 5$, $n^S = 0$ lines. An intensity calculation (Section IV(C)) shows the unobserved transitions to have low intensity for the excitation sequence used. The theoretical stick spectrum, with line intensities adjusted for observed differences in experimental linewidths, is shown in Figure 8(b).

Figure 7(c) illustrates a simple pulse sequence for obtaining spectra characterized by $|n^I| \leq N$, $n^S = \pm 1$, while the sequence in Figure 7(d) incorporates a pulsed field gradient to select a particular proton order. As will be discussed in Section IV(D), one generally expects to excite both $n^S = \pm 1$ and $n^S = 0$ lines with these sequences. The spectrum obtained for $n^I = 5$, $n^S = 0, \pm 1$ is shown in Figure 9, with line positions and assignments for this spectrum tabulated in Table I.

B. Excitation period decoupling

A significant feature of the pulse sequences of Fig. 7 is the use of ^{13}C decoupling during the excitation (preparation and mixing) periods. This has a number of advantages. By removing one spin from the excitation dynamics, the size of the Liouville space available to the density operator is reduced. Table II demonstrates one consequence of this reduction. The

sum of the line intensities within each order n^I has been calculated for [1 - ^{13}C] benzene with and without ^{13}C decoupling. The tabulated numbers are integrals over the excitation variable τ .[38] The ^{13}C decoupling on average increases the $n^I = 6$ and $n^I = 5$ intensities by factors of 3.1 and 1.1, respectively. This enhancement of the highest order coherence is particularly large for a molecule like [1-^{13}C] benzene, where the symmetry is, in effect, increased by ^{13}C decoupling.

The ^{13}C decoupling also simplifies considerably the search for particularly favorable values of τ . This is because the number of eigenfrequencies contributing to the excitation dynamics is reduced and, more importantly, because the signal during the search procedure comes from unlabeled molecules as well as those containing a ^{13}C nucleus. This would be particularly important with natural abundance samples and when there are many distinct ^{13}C sites, since the same excitation sequence suits all isomers. A search procedure for excitation sequences is discussed elsewhere.[39]

C. Intensity calculation for the high order $n^S = 0$ spectra

The excitation period decoupling also simplifies the intensity calculation. Most importantly, in certain cases it allows the intensities of the transitions of the labeled molecules to be related to one another and to those of the unlabeled molecules, regardless of the details of the excitation periods. Such intensity

calculations are an aid in line assignments. The principles are illustrated here by the calculation of the relative intensities of the $n^I = 5$, $n^S = 0$ transitions shown in Fig. 8(b) and obtained with the pulse sequence of Fig. 7(b).

There are only two $n^I = 5$ coherences for the decoupled [1 - ^{13}C] benzene molecules or equivalently for the unlabeled molecule. These are known by symmetry to be associated with the operators:

$$X_\alpha^5 = \sum_i I_{0i}^+ \prod_{j\neq i} I_{+j} = \frac{1}{2}|m^I = 3 >< m^I = -2, A_1(^{12}C)| \qquad (17a)$$

$$X_\beta^5 = \sum_i I_{0i}^- \prod_{j\neq i} I_{+j} = \frac{1}{2}|m^I = 2, A_1(^{12}C) >< m^I = -3| \quad . \qquad (17b)$$

The notation in the outer products specifies the proton Zeeman quantum number, the irreducible representation, and the applicable permutation group, which is labeled by ^{12}C or ^{13}C to indicate that the group is assumed to change to that of the unlabeled molecule when the ^{13}C is decoupled. For the case of [1 - ^{13}C] benzene the group is C_2 and effectively reverts to D_6 under decoupling. The factor of 1/2 keeps the normalization consistent with the undecoupled operators and may also be written as $(1/2)(S_0^+ + S_0^-)$.

At $t_1 = 0$ the Hamiltonian suddenly changes to $\mathcal{H}_1$. For the experimental sequences of Fig. 7,

$$\mathcal{H}_1 = \mathcal{H}_{II} + \mathcal{H}_{IS} \qquad (18)$$

since Zeeman terms are effectively removed by the π pulses at at $t_1/2$. The eigenoperators under the Hamiltonian of Eq. (18) with $n^I = 5$ and $n^S = 0$ are

$$X^5_{\alpha,\pm}(^{13}C) = S^{\pm}_0 \, |m^I = 3 >< m^I = -2, A_1(^{13}C), \alpha, \pm 1| \qquad (19a)$$

$$X^5_{\beta,\pm}(^{13}C) = S^{\pm}_0 \, |m^I = 2, A_1(^{13}C), \beta, \pm >< m^I = -3| \quad . \qquad (19b)$$

The eigenstates with index of α or β (running from 1 to 4) must be calculated numerically by 4 x 4 diagonalizations within the totally symmetric $|m^I| = 2$, $|m^S| = 1/2$ manifolds (Figure 6). The plus sign refers to the $m^S = 1/2$ manifold and the minus sign to $m^S = -1/2$.

The relative intensity of the observed $n^I = 5$, $n^S = 0$ lines can now be calculated in terms of the inner products of the decoupled eigenoperators. The ratio of the intensity of a transition of the ^{13}C-containing molecules to the corresponding transition of the unlabeled molecules can be expressed in terms of the mole fraction χ_{13} of labeled molecules and quantum mechanical traces as:

$$\frac{|I^5_{\alpha,\pm}(^{13}C)|}{|I^5_{\alpha}(^{12}C)|} = \frac{\chi_{13}|\mathrm{Tr}(X^5_{\alpha,\pm}(^{13}C))^{\dagger} X^5_{\alpha}(^{12}C)|^2}{(1-\chi_{13})|\mathrm{Tr}(X^5_{\alpha}(^{12}C))^{\dagger} X^5_{\alpha}(^{12}C)|^2} \quad . \qquad (20)$$

Since the $|m^I| = 3$ eigenstates are the same with and without decoupling, the traces can be simplified to

$$\frac{|I^5_{\alpha,\pm}(^{13}C)|}{|I^5_{\alpha}(^{12}C)|} = \frac{\chi_{13}}{(1-\chi_{13})} \; \frac{1}{2}|<m^I = -2, A_1(^{13}C), \alpha, \pm|m^I = -2, A_1(^{12}C)>|^2 \quad . \qquad (21)$$

By the completeness property, there is a sum rule:

$$\sum_{\alpha=1}^{4} \sum_{\pm} \frac{|I^5_{\alpha,\pm}(^{13}C)|}{|I^5_{\alpha}(^{12}C)|} = \frac{\chi_{13}}{(1-\chi_{13})} \quad . \tag{22}$$

This simply states that the total intensities from the labeled and unlabeled molecules are in proportion to their mole ratio. This would not be the case had $\mathcal{H}_{IS}$ played a role in the excitation dynamics.

Analogous expressions hold for the transitions indexed by β . The resulting intensities for the lines of Fig. 8(a) are shown as a stick spectrum in Fig. 8(b). The theoretical sum of the intensities in the five unobserved pairs is 8% of the total intensity.

A similar, but simpler, analysis gives the relative intensities of the $n^I = 6$, $n^S = 0$ transitions also shown in Fig. 8. The sum of the satellites is again related to the central transition from the unlabeled molecules by their respective mole fractions.

D. Two step excitation of $n^S = 1$ coherence

The density operator prepared from I magnetization with S decoupling contains only coherences with $n^S = 0$. In order to introduce $n^S = \pm 1$ terms, two additional requirements must be met.

First, $\mathcal{H}_{IS}$ must be allowed to act for a period of time $\tau_{IS} \gtrsim F_{iS}^{-1}$, and then an S pulse is applied in order to change the quantum number n^S of the HMQ coherence from zero to ± 1. Prior to the action of $\mathcal{H}_{IS}$, this pulse would have no effect since the S spin factor in each coherence is proportional to the identity $(S_0^+ + S_0^-)$.

When $\mathcal{H}_{II}$ is present along with $\mathcal{H}_{IS}$ during the period τ_{IS}, as in Figs. 7(c) and (d), then the dynamics of the transfer of coherence to $n^S = \pm 1$ requires numerical calculation for a general value of n^I. A special case however is the $n^I = N$ coherence. As noted in connection with Eq. (14), this eigenoperator evolves according to the sum $\sum_i F_{iS}$ regardless of $\mathcal{H}_{II}$. Thus, if at the time the decoupling is discontinued the $n^I = N$ coherence is given by

$$\rho_{N,0}(\tau) = \frac{1}{2}(S_0^+ + S_0^-) \prod_i I_{+i} \quad , \tag{23}$$

then at time τ_{IS} later it is given by

$$\rho_{N,0}(\tau + \tau_{IS}) = \frac{1}{2}(S_0^+ \exp(i\theta_{IS}) + S_0^- \exp(-i\theta_{IS})) \prod_{i=1}^{N} I_{+i} \tag{24}$$

where $\theta_{IS} = 2\pi\tau_{IS} \sum_i F_{iS}$. For $\theta_{IS} = \pi/2$ this is

$$\rho_{N,0}(\tau + |4\textstyle\sum_i F_{iS}|^{-1}) = S_Z \prod_i I_{+i} \quad . \tag{25}$$

A $\pi/2$ pulse at the S Larmor frequency converts this into

$n^I = N$, $n^S = \pm 1$ coherence with complete efficiency. As noted in Section III(B) this coherence is invariant to both $\mathcal{H}_{II}$ and $\mathcal{H}_{IS}$ and thus gives a central peak under the Hamiltonian of Eq. (18). Equation (25) was confirmed by completely transferring the $n^I = 6$, $n^S = 0$ ^{13}C satellites of Fig. 8(a) into the central line when τ_{IS} was set equal to half the inverse of the satellite splitting.

The same pulse sequences also result in $n^S = \pm 1$ spectra for other values of n^I (Fig.(9) and Table I). For these lines even a relative intensity calculation would require a numerical dynamical calculation. Thus the assignments of Table I were made on the basis of frequency alone.

V. Scalar Heteronuclear Recoupled Interactions by Multiple Pulse (SHRIMP)

A. Motivation

In Section III the spectrum of the higher order HMQ coherences was discussed for an effective evolution Hamiltonian (Eq. 13) from which $\mathcal{H}_{II}^D$ had been removed. A common feature of all published pulse sequences designed to remove $\mathcal{H}_{II}^D$ is that they result in a scaling of the heteronuclear interactions $\mathcal{H}_{IS}$ by a factor $K \leq 1/\sqrt{3}$. A similar scaling of the I spin chemical shift terms is a necessary corollary of removing $\mathcal{H}_{II}^D$. The scaling of $\mathcal{H}_{IS}$, however, is not necessary and for our purposes here such a scaling is undesirable, since it reduces the effective magnitude of the interactions being measured.

In this section we introduce the concept of scalar hetero-

nuclear recoupled interactions by multiple pulse (SHRIMP), which allows the measurement of $\mathcal{H}_{IS}$ without scaling, while still removing $\mathcal{H}_{II}^{D}$. Additional advantages of the method are that it leads to HMQ spectra with properly phased lines having relative intensities which are independent of the excitation dynamics and easily calculated.

B. The SHRIMP sequence

The trick to removing $\mathcal{H}_{II}^{D}$ without scaling down $\mathcal{H}_{IS}$ is simply to give the same pulses to the S spin as to the I spins. This keeps the two sets of angular momentum components always parallel in the toggling frame. If we also require that the Zeeman terms $\mathcal{H}_{I}^{Z}$ and $\mathcal{H}_{S}^{Z}$ vanish, then the desired average Hamiltonian for the SHRIMP sequences is

$$\mathcal{H}_{I\cdot S} + \mathcal{H}_{II}^{J} = \sum_{i} 2F_{iS}\, \underset{\sim}{I}_{i}\cdot\underset{\sim}{S} + \sum_{i<j} J_{ij}\, \underset{\sim}{I}_{i}\cdot\underset{\sim}{I}_{j} \quad . \tag{26}$$

The first term is the average Hamiltonian resulting from $\mathcal{H}_{IS}$. The notation $\mathcal{H}_{I\cdot S}$ indicates that the interaction has taken on the operator form of scalar coupling in spin space. This amounts to a recoupling of the I and S nuclei so that flip-flop terms normally suppressed by the large differences in Larmor frequencies, are reintroduced.

A particular pulse sequence which leads to the average Hamiltonian of Eq. (26) is that described in the ABC notation[40] as

$$(ABC)(C\bar{B}\bar{A})(\bar{A}B\bar{C})(\bar{C}\bar{B}A)(A\bar{B}\bar{C})(\bar{C}B\bar{A})(\bar{A}\bar{B}C)(CBA) \qquad (27)$$

The letters indicate the toggling frame value of $U_{rf}^{-1}(I_Z + S_Z)U_{rf}$ and specify a sequence in which the same pattern of rf pulses is given to both the I and S spins. The sequence consists only of $\pi/2$ pulses and is compensated to give no contribution from $\mathcal{H}_{II}^{D}$ to the average Hamiltonian even for finite pulse length. Since it is symmetric, $\mathcal{H}^{(1)}$ correction terms also vanish.[11]

C. Evolution under SHRIMP

The average Hamiltonian of Eq. (26) has fundamentally different properties than either the unperturbed Hamiltonian of Eq. (1) or the previous multiple pulse Hamiltonian of Eq. (13). The Zeeman quantum numbers of the individual spin species are not conserved. However, it is true that

$$[\underset{\sim}{I} + \underset{\sim}{S}\ ,\ \mathcal{H}_{I\cdot S} + \mathcal{H}_{II}^{J}] \ = \ 0 \qquad . \qquad (28)$$

This implies that the sum of the Zeeman quantum numbers is conserved and, in addition, that the Hamiltonian is isotropic in spin space. The principal consequence for HMQ experiments is that the sum

$(n^I + n^S)$ is conserved, though not the individual quantities.

An interesting consequence of Eq. (28), which will not be pursued here, is that the SHRIMP sequence could serve as a cross polarization scheme. It transfers any component of I magnetization to the corresponding component of S in much the same way that Hartmann-Hahn cross polarization[41] transfers the spin locked component.

D. HMQ spectroscopy under SHRIMP

In this section we discuss the consequence of using Eq. (26) as the evolution period Hamiltonian $\mathcal{H}_1$ of Fig. 5. Figure 10 shows the energy level diagram relevant to the high order HMQ spectroscopy of [1 - ^{13}C] benzene under the SHRIMP Hamiltonian of Eq. (26). Unlike the situation depicted in Fig. 6, subspectral analysis is not applicable. The total spin transition characterized by $(n^I + n^S) = 7$ is still independent of all couplings between spins.

The transitions characterized by $(n^I + n^S) = 6$ belong to the A irreducible representation, since they involve the totally symmetric states with $m^I + m^S = 7/2$. There are apparently five pairs of such transitions, but in fact one pair has no splitting and constitutes a degenerate central line. This is not peculiar to this molecule, but is in fact a general feature which follows from the commutator of Eq. (28). To see this, consider the operator formed from the total spin coherence operator by the action of the lowering derivation-superoperator $(I_- + S_-)$, :[42]

$$[(I_- + S_-),\ S_+ \prod_i I_{+i}] = S_0^- \prod_i I_{+i} + S_+ \sum_i (I_{0i}^- \prod_{j \neq i} I_{+i}) \quad (29)$$

This is evidently an $(n^I + n^S) = N$ operator. Its commutator with the Hamiltonian of Eq. (26) is however zero, as is most easily seen by noting that both terms on the left of Eq. (29) do so commute. This argument can be extended by induction to prove that there is a center line for every order $(n^I + n^S)$.

In general then, there are as many pairs of $(n^I + n^S) = N$ transitions containing information on $\mathcal{H}_{I\cdot S} + \mathcal{H}^J_{II}$ as there are distinct I spins. This number is N for an unsymmetrical molecule and 4 for [1 - ^{13}C] benzene. This is also the number of unknown parameters F_{iS}. The question then arises of how the corresponding coherence can be excited. For the same reasons as discussed in Section IV(B), it is desirable to use S spin decoupling during preparation and mixing periods. Thus it is reasonable to consider as an initial condition at $t_1 = 0$ the $n_S = 0$ operators prepared with decoupling.

The simplest initial condition is the operator with $n_I = N$:

$$\rho(t_1=0) = X^N = \frac{1}{2}\prod_i I_{+i} \quad . \tag{30}$$

During the evolution period this will evolve into other operators with $(n^I + n^S) = N$ so that at time t_1 additional terms of order $(n^I = N - 1, n^S = 1)$ will be present. However these need not lead to I magnetization in t_2, since decoupling will tend to destroy any $n^S = 1$ coherence and order specific selectivity[43] in the mixing period will discriminate against $n^I \neq N$ coherence. With these considerations it is possible to write the SHRIMP

interferogram with initial condition $n^I = N$ as the autocorrelation function $Tr(X^{N^\dagger}(0)X^N(t_1))$. The fact that the signal can be written as a single autocorrelation function guarantees that the lines will all appear with the same phase. The intensities are found to be, in analogy to Eq. (20):

$$\frac{|I^N_{\alpha,\pm}(^{13}C)|}{|I^N(^{12}C)|} = \frac{\chi_{13}}{(1-\chi_{13})} \frac{1}{2}|\langle m^I + m^S = \pm\frac{(N-1)}{2}, A_1(^{13}C),\alpha | m^I = \pm\frac{N}{2}, m^S = \frac{-1}{+2}, A_1(^{12}C)\rangle|^2 \quad . \tag{31}$$

A sum rule identical to Eq. (22) holds. Here α labels as many distinct pairs as there are distinct I spins, plus one. The $\pm$ sign distinguishes members of a pair, but they have identical intensities. As noted, one pair falls at the center and is thus degenerate with the signal from the unlabeled molecules. The other pairs, in principle, are sufficient to determine the unknowns F_{iS}.

VI. Spreading Parameters in HMQ Spectroscopy with I Spin Detection

A. Motivation and Introduction

The discussion so far has been for a single system of N spins I and one spin S. In some situations, most notably that in which S represents ^{13}C at natural abundance, the sample consists of a collection of such systems. In such a case it is important to be able to distinguish the transitions arising from each system. An effective way of doing this is to introduce a period in which the

dynamics are determined by the chemical shift or quadrupole coupling of the S spin. These serve as spreading parameters which separate the spectra of the various systems and facilitate their assignment to particular molecular species.

Because of the reduced signal-to-noise ratio associated with direct observation of the S spin, it is advantageous to introduce the evolution due to $\mathcal{H}_S^Z$ or $\mathcal{H}_S^Q$ into the evolution period. This can be done by following the evolution of an $n^S = \pm 1$ HMQ operator, but detecting I spin magnetization in t_2. Such an indirect measurement of $\mathcal{H}_S^Z$ has been demonstrated in the liquid state spectrum of $^{13}CH_3I$.[27]

In the evolution sequences discussed in the previous sections for which $n^S = \pm 1$ HMQ coherence was considered, the emphasis was on the dipolar evolution and the Zeeman term $\mathcal{H}_S^Z$ was intentionally suppressed in the interest of removing the effect of magnet inhomogeneity. In this section we indicate how the previous sequences may be augmented to achieve separation of the spectra arising from different species according to $\mathcal{H}_S^Z$ or $\mathcal{H}_S^Q$. This can be done with a sequence which remains immune to inhomogeneity of Zeeman terms and, in addition, suppresses the signal from species which do not contain an S spin.

Experiments which begin by preparing the total spin coherence ($n^I = N$) of the I spin system are of particular interest. As discussed in Section IV(D), this term can be quantitatively converted into ($n^I = N$, $n^S = \pm 1$) coherence and also (Section V) serves as the initial condition for SHRIMP evolution. Figures 11(a) and (b) depict pulse sequences designed to measure the quantity $\sum_i F_{iS}$ for each

S spin and to correlate it with the chemical shift ν_S or quadrupole coupling ν_Q of that spin. These serve as prelude to the sequence of Fig. 11(c) in which both $\sum_i F_{iS}$ and ν_S are used to identify the HMQ transitions of the species containing that S spin.

A common feature of all of these sequences is that the evolution period is divided into two parts

$$t_{1a} + t_{1b} = t_1 \quad . \tag{32}$$

In a given experiment the ratio t_{1a}/t_{1b} is held fixed as t_1 increases. The particular ratio used is chosen so as to allow resolution of all frequencies appearing in the Fourier transformation with respect to t_1.

B. Correlation of $\sum_i F_{iS}$ with ν_S or ν_Q

Each of the sequences of Fig.(11) begins with the preparation of $(n^I = N, n^S = 0)$ coherence under the preparation propagator U. In the first experiment (Fig. 11(a)) this evolves according to $\sum_i F_{iS}$ (Eq. 14) for time $t_{1a}/2$, is converted to $(n^I = N, n^S = \pm 1)$ coherence for a time t_{1b}, and then back to $n^S = 0$ for a second period $t_{1a}/2$ before mixing to observable I magnetization.

The I spin π pulse during t_{1b} refocuses that coherence which spends time xt_{1b} with quantum numbers $(n^I = N, n^S = -1)$ and time $(1 - x)t_{1b}$ with $(n^I = -N, n^S = -1)$. The fraction x, given by

$$x = (N\gamma_I + \gamma_S)/2N\gamma_I \quad , \tag{33}$$

is chosen to remove the effects the inhomogeneous Zeeman terms involving $\nu(\underset{\sim}{r})$ (Eq. 2) only for this coherence. Other coherence, including all that arising from systems unlabeled by an S spin, may be suppressed by intentionally increasing the range of $\nu(\underset{\sim}{r})$ with a pulsed field gradient during t_{1b}. As demonstrated below, further suppression of unwanted coherence may be achieved by shifting the relative phase of the S spin pulses in successive shots.[31-33]

For S = 1/2, the spectrum resulting from Fourier transformation with respect to t_1 is a triplet centered at

$$\frac{t_{1b}}{t_1}((-\nu_S - \Delta\nu_S) + (\gamma_S/\gamma_I)\Delta\nu_I) \quad . \tag{34}$$

The splitting between the outer lines of this triplet is

$$\frac{t_{1a}}{t_1} \left| \sum_i F_{iS} \right| \quad . \tag{35}$$

This allows association of $\sum_i F_{iS}$ for a particular S spin with that spin's chemical shift, ν_S.

This was demonstrated on the same sample of enriched [1 - ^{13}C] benzene using the pulse sequence of Figure 11(b). T and τ' were chosen so that only $n^I = 6$ coherence is echoed. Four different experiments were performed, the phase of the first S-spin $\pi/2$ pulse being incremented by 90° with each successive experiment. Data from these four experiments were combined so that only the triplet of lines belonging to $n^S = -1$ coherence was retained. The effect of S-spin chemical shift was simulated by changing the ^{13}C synthesizer frequency. Figure 12(a) shows the positions of the triplet lines,

as a function of ^{13}C frequency offset, with the proton frequency set on resonance. As expected, these lines move in unison as the frequency is varied, the change in line position with changing offset frequency being determined by the ratio $t_{1b}/t_1 = 0.49$ through Eq. (34). Figure 12(b) shows similar results of experiments in which the ^{13}C frequency is set on resonance and the proton offset frequency varied. Again Eq. (34) is confirmed. Finally, the effect of changing the ratio t_{1a}/t_1 (Eq. 35) is illustrated in Figure 12(c). The results of these experiments demonstrate that by an appropriate choice of the ratio t_{1a}/t_1, separated triplets could be obtained, and $\sum_i F_{iS}$ correlated with ν_S, even for several inequivalent S spins, without detecting S magnetization.

C. Sorting of HMQ spectra by spreading parameter

The correlation of $\sum_i F_{iS}$ with ν_S is useful in choosing the parameter τ_{IS} in the sequence of Figure 11(c). This sequence begins with evolution of $n^I = N$ coherence under, for example, the SHRIMP Hamiltonian of Eq. (26) for a time t_{1a}. After a $\pi/2$ S pulse, evolution for time t_{1b}, as in the sequence of Fig. 11(a) shifts the SHRIMP spectrum for each spin a distance proportional to ν_S. As t_1 is incremented the time τ_{IS} is held fixed. In the Fourier transform with respect to t_1, a given set of SHRIMP lines, corresponding to the heteronuclear couplings to a particular S spin, varies as $\sin(\theta_{IS})$ as described by Eq.(24). A pulsed field gradient during t_{1b} and/or phase shifting of S

spin pulses can again be used to suppress unwanted coherence.

VII. CONCLUSION

The measurement of nuclear dipolar couplings in molecules containing a rare and an abundant spin species has been reexamined and several new approaches demonstrated. The exponential increase in spectral complexity with system size is a problem which was unsolved even by single quantum local field methods. The multiple quantum methods demonstrated should allow spectroscopy at the resolution of single transitions for larger molecules than is otherwise possible.

The rationale for removing the effect of the homonuclear dipolar couplings from the spectra still remains, though, even when high order multiple quantum coherence is observed. This removal reduces the number of unknowns and in many cases will improve the magnetic isolation that makes high resolution possible. The usual approach is to irradiate only the abundant nuclei with a multiple pulse line narrowing sequence. A new approach (SHRIMP) was introduced here which entails irradiation of both species. This eliminates the undesirable scaling down of the heteronuclear couplings which are to be measured.

Another desirable feature of any experiment designed for large molecules is that it generates spectra whose relative intensities can be readily simulated. In general, this becomes difficult in multiple quantum experiments, because of the complex dynamics of the excitation periods. The elimination of this problem by the separation of homonuclear and heteronuclear excitation was demonstrated for the high order spectra of [1-^{13}C] benzene. For the $n^I = 5$ spectrum this

calculation depended on the high molecular symmetry. Both the SHRIMP method and total spin coherence transfer echo spectroscopy (TSCTES) discussed elsewhere[35,43] lead to relative line intensities independent of the excitation periods for any symmetry. TSCTES also should find application in heteronuclear systems.

In all the experiments discussed the final detection of magnetization is at the abundant spin frequency, since this typically gives greater sensitivity. Optimization of sensitivity will frequently require selective excitation of high order coherence[44] exactly as in purely homonuclear experiments. The methods demonstrated in Section VI allow the spectra to be labeled with the resonance frequency of the low sensitivity heteronuclear spin, although it is never directly observed.

Acknowledgements

The authors gratefully acknowledge the assistance of Steve Sinton and Jim Murdoch in the computer simulations and of Dione Carmichael in the preparation of this manuscript. This work was supported by the Director, Office of Energy Research, Office of Basic Energy Sciences, Materials Sciences Division of the U.S. Department of Energy under Contract Number DE-AC03-76SF00098.

Figure 1: Schematic representation of the single quantum random local field and multiple quantum ordered local field for a system of one ^{13}C and N protons. (a) In the single quantum experiment the protons are assumed to be uncoupled from one another. A total of 2^N different proton configurations are possible, one of which is shown. The ^{13}C heteronucleus may experience any of these different proton local fields. (b) In the heteronuclear multiple quantum experiments the protons are excited as a coherent group. One of the six possible groups of 5 protons is illustrated. This fewer number of ordered local fields enhances spectral resolution by reducing the number of possible transition frequencies. These frequencies measure sums and differences of individual heteronuclear couplings, thus providing information on relative signs to which the single quantum spectra are insensitive.

Figure 2: Graph of $\log_{10}$ (number of spectral lines) vs. number of I spins (N) for the I spin single quantum spectrum (O), the S spin single quantum spectrum (□), and the (n^I = N-1, n^S = 0) HMQ spectrum (Δ). (a) $\mathcal{H}_{II} \neq 0$, the case in which homonuclear dipolar couplings are not removed or scalar spin-spin couplings are not negligible. The number of single quantum transitions in either the I or S spectrum increases by about a factor of 4 for each additional I spin. In contrast, the number of (N-1) quantum lines varies only linearly with N. (b) In the absence of any homonuclear couplings ($\mathcal{H}_{II} = 0$), the single quantum proton and (n^I = N-1, n^S = 0) spectra contain the same number of lines (2N).

The line density of the single quantum S spectrum still grows exponentially, doubling for each additional I spin. Although this limit of $\mathcal{H}_{II} = 0$ is approached when $\mathcal{H}_{II}^{D}$ is removed in local field spectra, the scalar terms $\mathcal{H}_{II}^{J}$ prevent its precise realization.

Figure 3: Simulations of ^{13}C single quantum spectra of [1-^{13}C] benzene partially oriented in liquid crystal solvent. The parameters used are those of ref. (17), with all couplings expressed in Hz: $D_{12} = -403.854$, $D_{13} = -77.498$, $D_{14} = -50.257$, $D_{15} = -1119.617$, $D_{25} = -153.006$, $D_{35} = -39.280$, $D_{45} = -26.489$; $J_{12} = 7.549$, $J_{13} = 1.378$, $J_{14} = 0.650$, $J_{15} = 157.914$, $J_{25} = 1.052$, $J_{35} = 7.653$, $J_{45} = -1.257$. (a) Stick simulation of normal spectrum with $\mathcal{H}_{II}$ fully operative. The presence of homonuclear dipolar couplings makes extraction of heteronuclear coupling constants difficult. This difficulty increases rapidly with larger systems. (b) Stick simulation of local field spectrum with $\mathcal{H}_{II}^{D} = 0$. The multiple pulse scale factor is 1/3. Although the total number of transitions has been greatly reduced relative to part (a), the density of lines within each of the two well-resolved groups is comparable. As a consequence only the largest of the ^{13}C-H couplings is typically resolvable with attainable linewidths. The smaller heteronuclear couplings and proton-proton indirect couplings appear as a line broadening which decreases the measurement accuracy.

Figure 4: Simulation of ^{1}H single quantum spectra of partially

oriented [1-^{13}C]benzene. Parameters are again those of ref. (17).

(a) Local field spectrum with $\mathcal{H}_{II}^{D}$ = 0, multiple pulse scale factor = $1/\sqrt{3}$. The information content relative to the corresponding ^{13}C local field experiment (Fig. 3(b)) is considerably improved. The two largest F_{iS} are given by the position of the two rightmost multiplets. Still, the indirect ^{1}H-^{1}H couplings, which are responsible for the dense packing of spectral lines, limit the accuracy with which F_{iS} may be determined. This can be seen by comparison with (b) the hypothetical spectrum in the absence of all homonuclear couplings ($\mathcal{H}_{II}$ = 0). Note that the two smallest F_{iS} given by the two leftmost lines of (b) are only crudely measured by the position of the corresponding multiplet in (a).

Figure 5: Generalized schematic diagram of time domain heteronuclear multiple quantum NMR experiments. Combined coherences of the I-S system, which are prepared through the action of propagator U, evolve for a time t_1 under the Hamiltonian $\mathcal{H}_1$. Propagator V then mixes these coherences back into observable magnetization which is collected as signal during t_2. Fourier transformation with respect to t_1 yields various spectra containing lines at the characteristic frequencies of the I-S system.

Figure 6: [1-^{13}C] benzene energy level diagram. Energy levels are sorted by total proton Zeeman quantum number (m^I) and by ^{13}C Zeeman quantum number (m^S). This is useful in that both m^I and m^S are good quantum numbers for free evolution of the spin system. Subspectra characterized by specific values of

$n^I = \Delta m^I$ and $n^S = \Delta m^S$ may be separately excited or may be sorted out either by their characteristic modulation properties under phase shifts of the r.f. irradiation or by their dephasing and rephasing properties under field gradients. Subspectra with $n^S = 0$ correspond to vertical transitions while those with $n^S = \pm 1$ connect a state in the left hand column with one on the right.

Figure 7: Simple HMQ NMR Pulse Sequences.

(a) This pulse sequence results in excitation of coherences characterized by $n^S = 0$ and all values of $|n^I| \leq N$. ^{13}C decoupling during preparation and mixing serves to remove $\mathcal{H}_{IS}$ from the excitation dynamics. This simplifies the search for favorable values of the preparation time τ and may serve to increase the intensity of the highest multiple quantum orders. In addition, in molecules having inequivalent ^{13}C sites, the decoupling insures that all species will be equally excited (See Section IV(B)).

(b) The application of a pulsed magnetic field gradient (cross-hatched areas) causes only coherence characterized by a single n^I value to be echoed. The particular proton order which echoes is selected by choosing the times T and τ' according to $\tau' = |n^I|T$.

(c) This pulse sequence results in excitation of coherences characterized by $n^S = 0, \pm 1$. Following excitation of the protons with $\mathcal{H}_{IS}$ removed, ^{13}C decoupling is turned off and $\mathcal{H}_{IS}$ is allowed to act for a time $\tau_{IS} \gtrsim |\sum_i F_{iS}|^{-1}$. A $\pi/2$ pulse on the ^{13}C

spins then changes the n^S quantum number of the HMQ coherence from zero to ± 1. The mixing period reverses these steps, allowing detection of I magnetization in t_2.

(d) Again a pulsed gradient is added to suppress all signal except that corresponding to a particular proton order n^I.

Figure 8:

(a) $n^I = 5$, $n^S = 0$ and $n^I = 6$, $n^S = 0$ multiple quantum spectra of partially oriented [1 - ^{13}C] benzene enriched to 90% obtained using the pulse sequence of Fig. 7(b). The benzene was dissolved at 40 mole % in Eastman 15320 nematic liquid crystal. The sample used was approximately 5 mm in diameter and 7 mm long. Each spectrum is the average of sixteen 1024 point free induction decays acquired with a 2 second recycle delay. The mixing period τ' was less than $|n^I|T$ due to the slow rise time of the pulsed magnetic field gradient. For the $n^I = 6$ spectrum, $\tau = 5.000$ msec, $T = 1.000$ msec, $\tau' = 4.300$ msec and $\Delta t_1 = 100$ μsec. The $n^I = 6$ spectrum shows a doublet whose splitting is $2|\sum_i F_{iS}|$, independent of the ^{1}H - ^{1}H couplings. The central line in this spectrum is the total spin transition from non-^{13}C-containing molecules. The $n^I = 5$ spectrum was acquired with $\tau = 6.540$ msec, $T = 1.380$ msec, $\tau' = 5.404$ msec, and $\Delta t_1 = 100$ μsec. It consists of three pairs of lines from [1 - ^{13}C] benzene molecules and one pair from unlabeled molecules.

(b) Theoretical stick simulations of $n^I = 5$, $n^S = 0$ and $n^I = 6$, $n^S = 0$ spectra. These spectra were obtained using the same

spin-spin couplings as the simulation of Figure 4(a), with the dipole couplings being scaled to fit the experimentally observed splitting in the $n^I = 6$ spectrum. This simple scaling is sufficient, because the ordering of the benzene molecules in the nematic liquid crystal is describable by a single order parameter. Relative line intensities (integrated areas) have been calculated as described in Section IV(C). These were divided by the experimentally observed linewidths to give the heights used in the stick simulation.

Figure 9:

$n^I = 5$, $n^S = 0, \pm 1$ multiple quantum spectrum of partially oriented [1 - ^{13}C] benzene enriched to 90% obtained using the pulse sequence of Figure 7(d). This spectrum was recorded with $\tau = 6.540$ msec, $T = 1.380$ msec, $\tau' = 5.404$ msec, and $\Delta t_1 = 100$ μsec. The spectrum displayed here is an average of magnitude spectra obtained for five different values of τ_{IS}: 100 μsec, 200 μsec, 250 μsec, 300 μsec, and 350 μsec. Fifteen 1024 point free induction decays were recorded for each value of τ_{IS}. Line positions and assignments for this spectrum are tabulated in Table I.

Figure 10:

[1 - ^{13}C] benzene energy level diagram relevant to SHRIMP spectroscopy. During evolution under the SHRIMP pulse sequence the individual spin quantum numbers m^I and m^S, and hence the differences n^I and n^S, are not good quantum numbers of the system. The sums $(m^I + m^S)$ and $(n^I + n^S)$ are however conserved quantities. Consideration of this diagram is useful in predicting the number of pairs of lines

expected in the SHRIMP spectrum. As proven in the text, one pair of lines of every order ($n^I + n^S$) has no splitting and appears at the center of the spectrum.

Figure 11: Pulse Sequences for the Correlation of Heteronuclear Coupling Constants with a Spreading Parameter

(a) This pulse sequence allows correlation of $\Sigma_i F_{iS}$ with the chemical shift ν_S of the ^{13}C nucleus involved. The propagators U and V interconvert observable I magnetization with the coherence ($n^I = N$, $n^S = 0$). The system evolves freely during the time periods labeled $t_{1a}/2$. During t_{1b} a field gradient may be applied. With $x = \frac{N\gamma_I + \gamma_S}{2N\gamma_I}$ the combined effect of the $\pi/2$ ^{13}C pulses and the off-center ^1H π pulse is to create a coherence transfer echo which removes inhomogeneous broadening from the spectrum and, with large gradients, suppresses signal from non-^{13}C-containing molecules. The resulting spectrum is a triplet from each different ^{13}C site. The splitting within each triplet is proportional to $\Sigma_i F_{iS}$, its center is proportional to the chemical shift of the ^{13}C, ν_S.

(b) The actual pulse sequence used for correlation of $\Sigma_i F_{iS}$ with ν_S in a sample of partially oriented [1 - ^{13}C] benzene enriched to 90%. A pulsed magnetic field gradient (cross-hatched area) discriminates against all coherence not prepared as $n^I = N$. No field gradient was applied during t_{1b}. A series of four experiments were performed, the phase ϕ of the first ^{13}C $\pi/2$ pulse being incremented by 90° with each successive experiment. Addition

of signal from these four experiments with weights $\exp(i\phi)$ yields the expected triplet of lines from coherence which spent time xt_{1b} as $n^I = N$, $n^S = -1$, and time $(1-x)t_{1b}$ as $n^I = -N$, $n^S = -1$.

(c) This pulse sequence allows separation of SHRIMP spectra by the chemical shift of the ^{13}C involved. Again, the initial condition of interest is $n^I = N$, $n^S = 0$. During t_{1a} a SHRIMP sequence (not drawn) is applied. As in (a), the combination of hard pulses and a field gradient during t_{1b} creates a coherence transfer echo. The time period τ_{IS} is fixed, being chosen to be on the order of $|\Sigma_i F_{iS}|^{-1}$. The result of this sequence is a scaled SHRIMP spectrum for each ^{13}C nucleus whose center is shifted proportional to the chemical shift of that carbon.

Figure 12: Line positions as a function of $\Delta\nu_{^{13}C}$, $\Delta\nu_{^1H}$, and (t_{1a}/t_1) in $n^I = 6$, $n^S = -1$ spectra of partially oriented [1 - ^{13}C] benzene. The pulse sequence is that of Figure 11(b). As discussed in the text, the spectrum obtained in each experiment is a triplet of lines; the line position of each of these three lines is graphed. All spectra were acquired with $\tau = 4.304$ msec, $T = 1.025$ msec, and $\tau' = 4.266$ msec.

(a) $\Delta\nu_{^{13}C}$ Dependence: Line positions as a function of ^{13}C frequency offset with ^1H frequency set on resonance. Experiments were run with $t_{1a} = 100$ μsec, $t_{1b} = 96$ μsec. The slope of the least squares fit to the position of each spectral line is 0.488; the theoretical value is $(\Delta t_{1b}/\Delta t_1) = 0.490$ (Eq. 34).

(b) $\Delta\nu_{1_H}$ Dependence: Line positions as a function of ^1H frequency offset with ^{13}C frequency set on resonance. Experiments were run with Δt_{1a} = 100 μsec, Δt_{1b} = 96 μsec. The slope of the least squares fit to the position of each spectral line is 0.120; the theoretical value is $(\gamma_S/\gamma_I)(\Delta t_{1b}/\Delta t_1)$ = 0.122 (Eq. 34).

(c) (t_{1a}/t_1) Dependence: Line positions as a function of the ratio ratio (t_{1a}/t_1) with both ^{13}C and ^1H frequencies set on resonance. Δt_{1a} and Δt_{1b} (= $(\Delta t_1 - \Delta t_{1a})$) were varied from one experiment to the next to achieve the desired ratio. The center line, which contains no dipolar information, remains stationary as a function of the fraction (t_{1a}/t_1); the splitting between the outer lines of the triplet varies linearly with this parameter (Eq. 35).

References

1. J. W. Emsley and J. C. Lindon, NMR Spectroscopy Using Liquid Crystal Solvents (Pergamon, Oxford, 1975).
2. J. S. Waugh, Proc. Natl. Acad. Sci. 73, 1394 (1976).
3. R. K. Hester, J. L. Ackerman, V. R. Cross, and J. S. Waugh, Phys. Rev. Lett. 34, 993 (1975).
4. R. K. Hester, V. R. Cross, J. L. Ackerman, and J. S. Waugh, J. Chem. Phys. 63, 3606 (1975).
5. M. E. Stoll, A. J. Vega, and R. W. Vaughan, J. Chem. Phys. 65, 4093 (1976).
6. E. F. Rybaczewski, B. L. Neff, J. S. Waugh, and J. S. Sherfinski, J. Chem. Phys. 67, 1231 (1977).
7. R. W. Vaughan, Ann. Rev. Phys. Chem. 29,397 (1978).
8. A. Hohener, L. Muller, and R. R. Ernst, Mol. Phys. 38, 909 (1979).
9. M. G. Munowitz, R. G. Griffin, G. Bodenhausen, and T. H. Huang, J. Am. Chem. Soc. 103, 2529 (1981).
10. T. Terao, H. Miura, and A. Saika, J. Chem. Phys. 75, 1573 (1981).
11. U. Haeberlen and J. S. Waugh, Phys. Rev. 175, 453 (1968).
12. U. Haeberlen, High Resolution NMR in Solids, Selective Averaging (Academic, New York, 1976).
13. M. Mehring, High Resolution NMR Spectroscopy in Solids, (Springer, Berlin, 1976).
14. M. Lee and W. I. Goldberg, Phys. Rev. 140, A1261 (1965).
15. J. A. Reimer and R. W. Vaughan, Chem. Phys. Lett. 63, 163 (1979).

16. J. A. Reimer and R. W. Vaughan, J. Magn. Reson. 41, 483 (1980).

17. P. Diehl, H. Bösiger and H. Zimmermann, J. Magn. Reson. 33, 113 (1979).

18. T. W. Shattuck, Ph.D. Thesis, University of California, Berkeley (1976, published as Lawrence Berkeley Laboratory Report LBL-5458).

19. S. Vega, T. W. Shattuck, and A. Pines, Phys. Rev. A 22, 638 (1980).

20. P. Brunner, M. Reinhold, and R. R. Ernst, J. Chem. Phys. 73, 1086 (1980).

21. M. Reinhold, P. Brunner, and R. R. Ernst, J. Chem. Phys. 74, 184 (1981).

22. S. Vega, Phys. Rev. A 23, 3152 (1981).

23. M.E. Stoll, A.J. Vega, and R.W. Vaughan, Phys. Rev. A 16, 1521 (1977).

24. M.E. Stoll, A.J. Vega, and R.W. Vaughan, J. Chem. Phys. 67, 2029 (1977).

25. P.M. Henrichs and L.J. Schwartz, J. Chem. Phys. 69, 622 (1978).

26. A.A. Maudsley, A. Wokaun, and R.R. Ernst, Chem. Phys. Lett. 55, 9 (1978).

27. L. Müller, J. Am. Chem. Soc. 101, 4481 (1979).

28. V.W. Miner and J.H. Prestegard, J. Amer. Chem. Soc. 103, 5979 (1981).

29. Y.S. Yen and D.P. Weitekamp, J. Magn. Reson. 47, 000 (1982).

30. A. Minoretti, W. P. Aue, M. Reinhold, and R. R. Ernst, J. Magn. Reson. 40, 175 (1980).

31. A. Wokaun and R. R. Ernst, Chem. Phys. Lett. 52, 407 (1977).

32. G. Drobny, A. Pines, S. Sinton, D. P. Weitekamp, and D. Wemmer, Faraday Symp. Chem. Soc. 13, 49 (1979).

33. G. Bodenhausen, R. L. Vold, and R. R. Vold, J. Magn. Reson., 37, 93 (1980).

34. A. Bax, P. G. DeJong, A. F. Mehlkopf and J. Smidt, Chem. Phys. Lett. 69, 567 (1980).

35. D. P. Weitekamp, J. R. Garbow, J. B. Murdoch, and A. Pines, J. Am. Chem. Soc. 103, 3578 (1981).

36. W. S. Warren, private communication.

37. S. W. Sinton, Ph.D. Thesis, University of California, Berkeley (1981, published as Lawrence Berkeley Laboratory Report LBL-13604).

38. J. B. Murdoch, W.S. Warren, D.P. Weitekamp, and A. Pines, to be published.

39. D. P. Weitekamp, J. R. Garbow, and A. Pines, J. Mag. Reson., 46, 529 (1982).

40. D. P. Burum and W. K. Rhim, J. Chem. Phys. 71, 944 (1979).

41. S. R. Hartmann and E. L. Hahn, Phys. Rev. 128, 2042 (1962).

42. C. N. Banwell and H. Primas, Mol. Phys. 6, 225 (1962).

43. D.P. Weitekamp, J.R. Garbow, and A. Pines, to be published.

44. W. S. Warren, D. P. Weitekamp, and A. Pines, J. Chem. Phys. 73, 2084 (1980).

Table I: Positions and Assignments of Lines in the $n^I = 5$, $n^S = 0, \pm 1$ Spectrum of Partially Oriented [1 - ^{13}C] Benzene shown in Figure 9.*

Observed Line Position (Hz)	Theoretical Line Position (Hz)	Assignment
49	34	$n^S = 0$
176	168	$n^S = \pm 1$
879	892	$n^S = 0$
1133	1155	$n^S = \pm 1$
1651	1673	$n^S = 0$**
1739	1760	$n^S = \pm 1$
1788	1806	$n^S = \pm 1$
1886	1914	Unlabeled Molecules
2706	2733	$n^S = \pm 1$
3566	3600	$n^S = 0$

* All of the lines in this spectrum occur in pairs. Accordingly, only lines at frequencies greater than 0 Hz are recorded in this table.

** This line is assigned as $n^S = 0$ based on its frequency. Its intensity here is anomalously large, however, since it does not appear in Fig. 8.

Table II: Number of Coherences and Total Magnitude Averaged Over τ per Multiple Quantum Order for [1 - ^{13}C] Benzene With and Without ^{13}C Decoupling During Preparation and Mixing.

Multiple Quantum Order (n^I)	No. of Coherences		Total Magnitude Averaged over τ	
	Coupled	Decoupled	Coupled	Decoupled
6	1	1	0.197	0.601
5	8	2	0.804	0.905
4	38	12	2.399	3.287
3	120	34	5.946	6.005
2	263	79	11.517	11.728
1	416	116	17.252	17.090
0	210	40	7.797	4.555

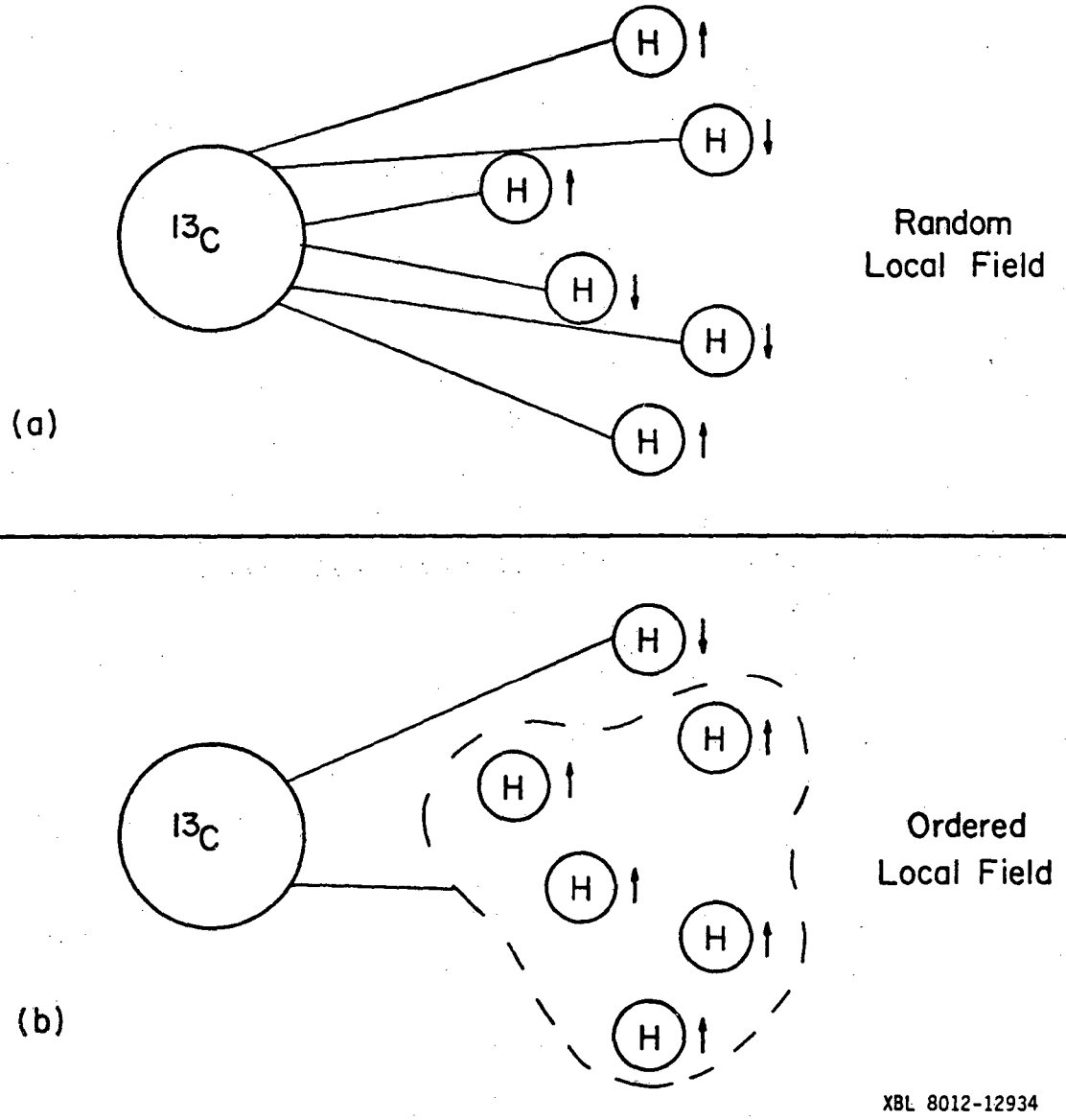
H
H
H
^{13}C
H
H
H
(a)
Random
Local Field
H
H
H
^{13}C
H
H
H
(b)
Ordered
Local Field
XBL 8012-12934

Figure 1

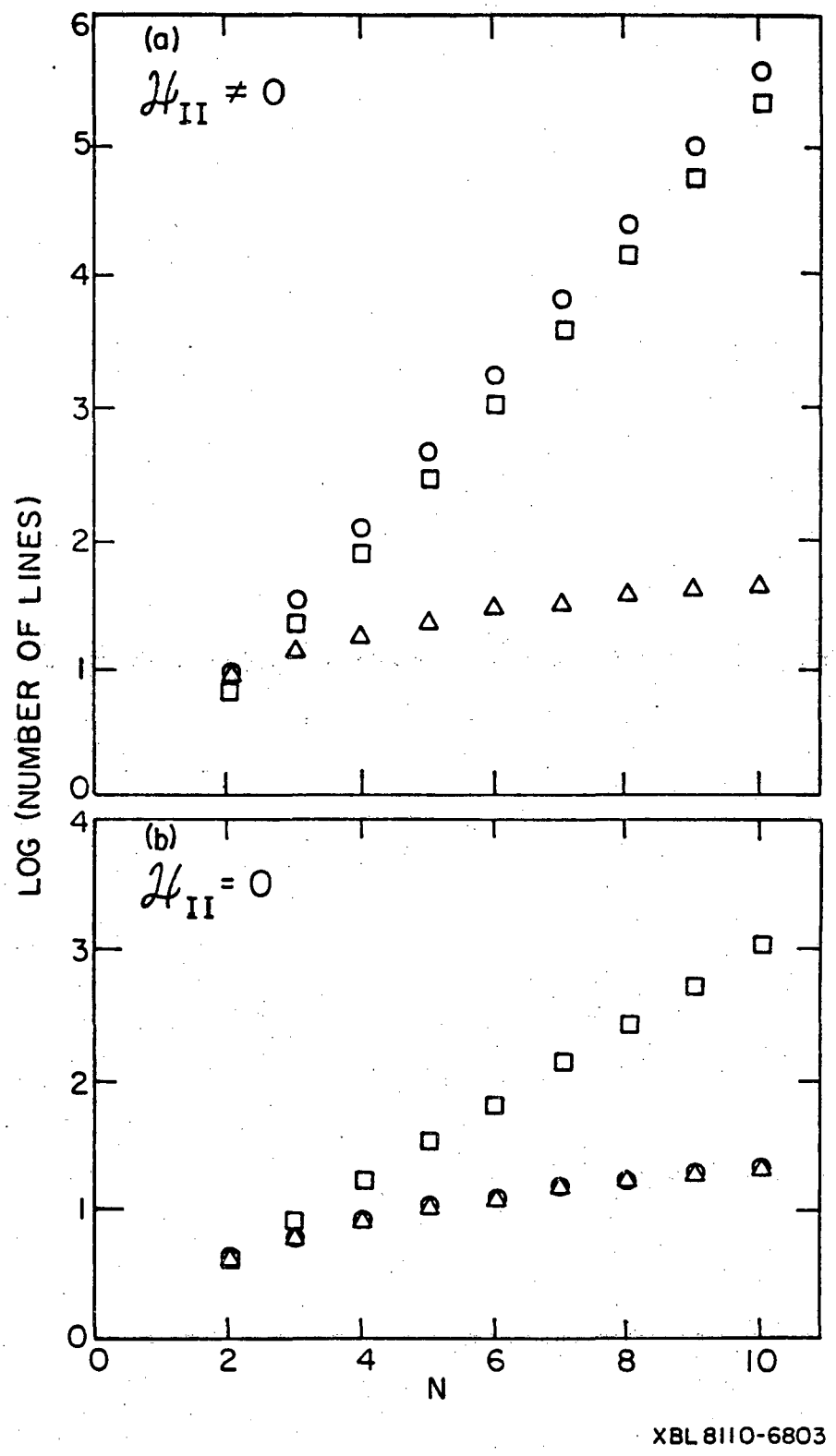
(a)
$\mathcal{H}_{II} \neq 0$
(b)
$\mathcal{H}_{II} = 0$
LOG (NUMBER OF LINES)
N
0
1
2
3
4
5
6
0
2
4
6
8
10
XBL 8110-6803

Figure 2

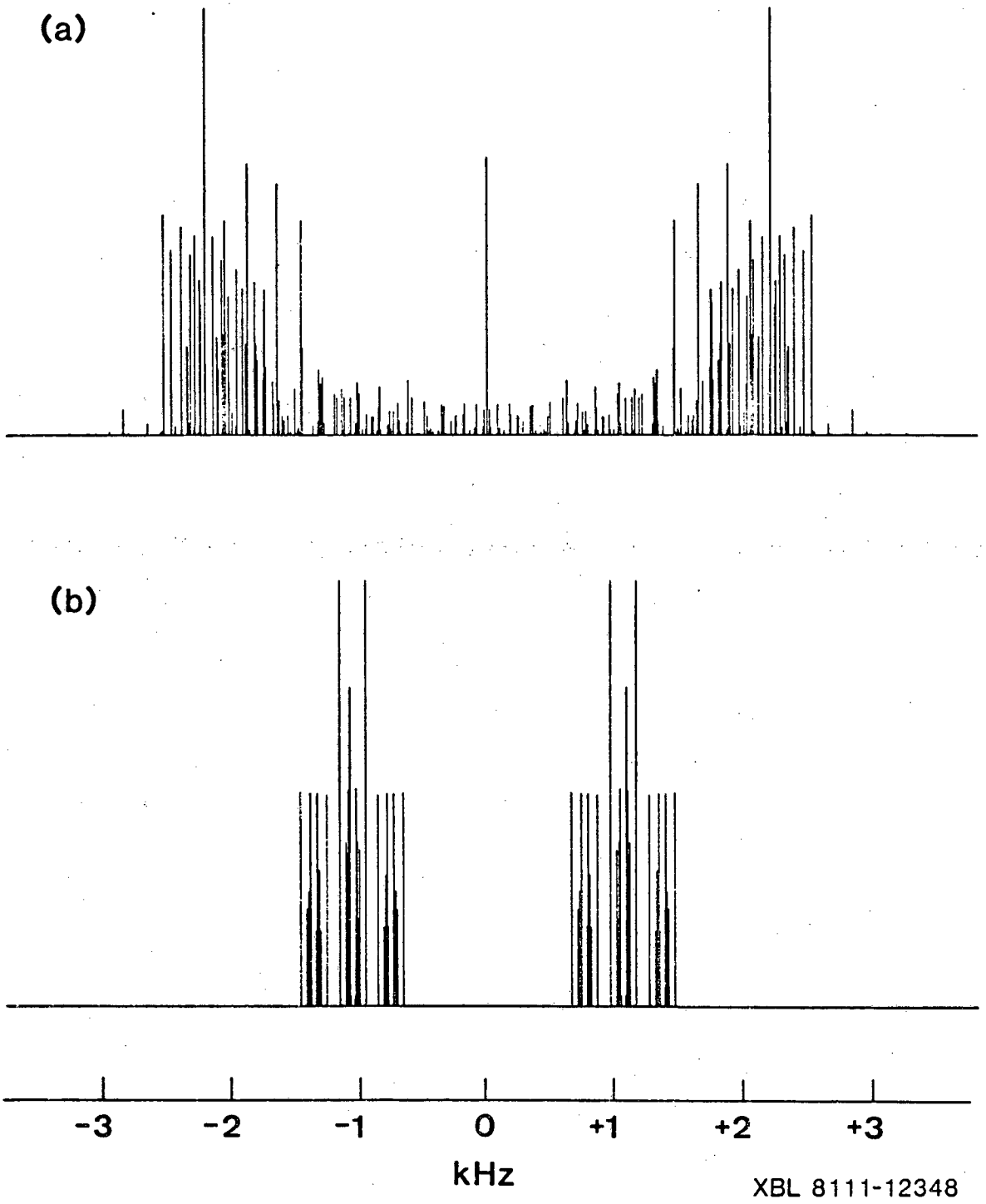

Figure 3

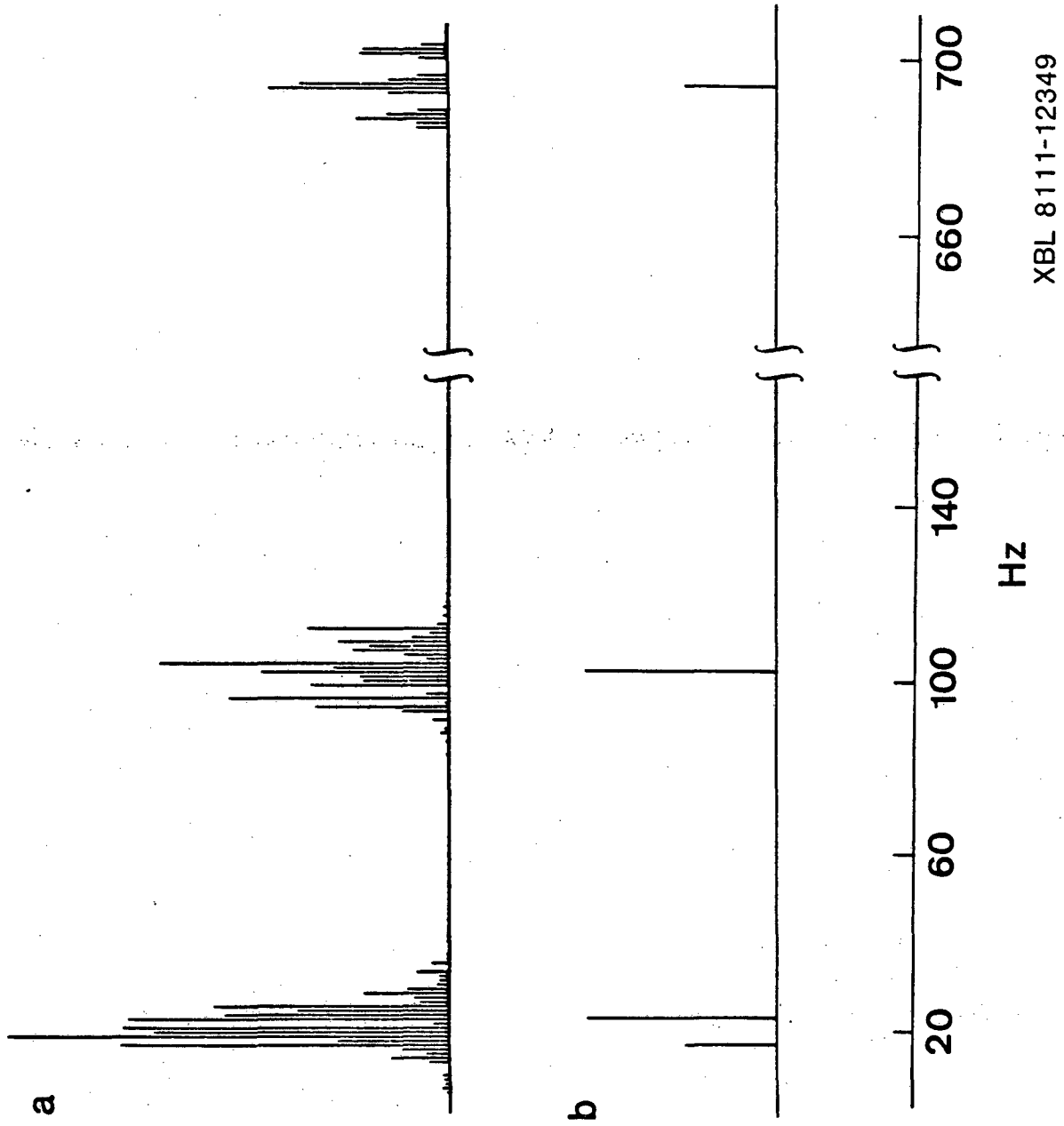

Figure 4

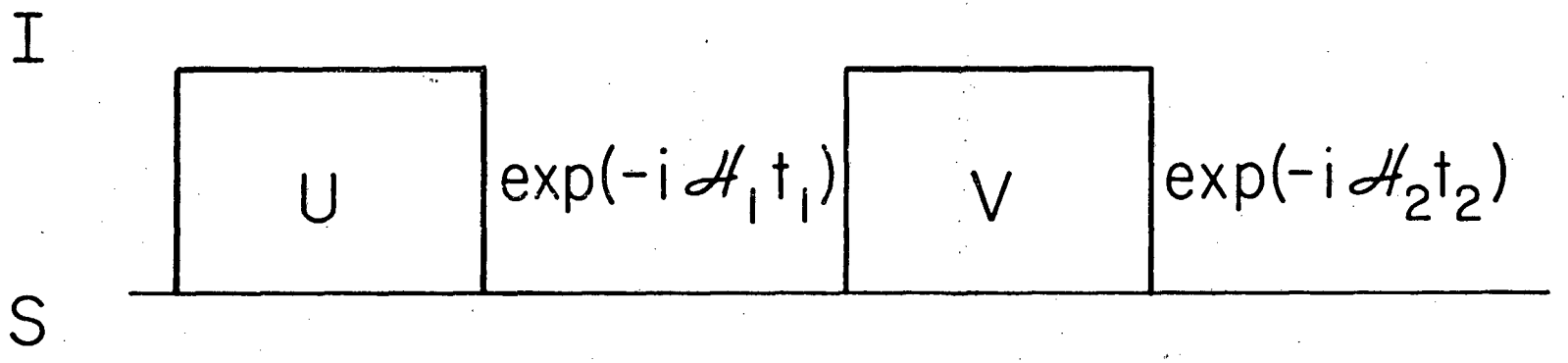

XBL 8110-7177

Figure 5

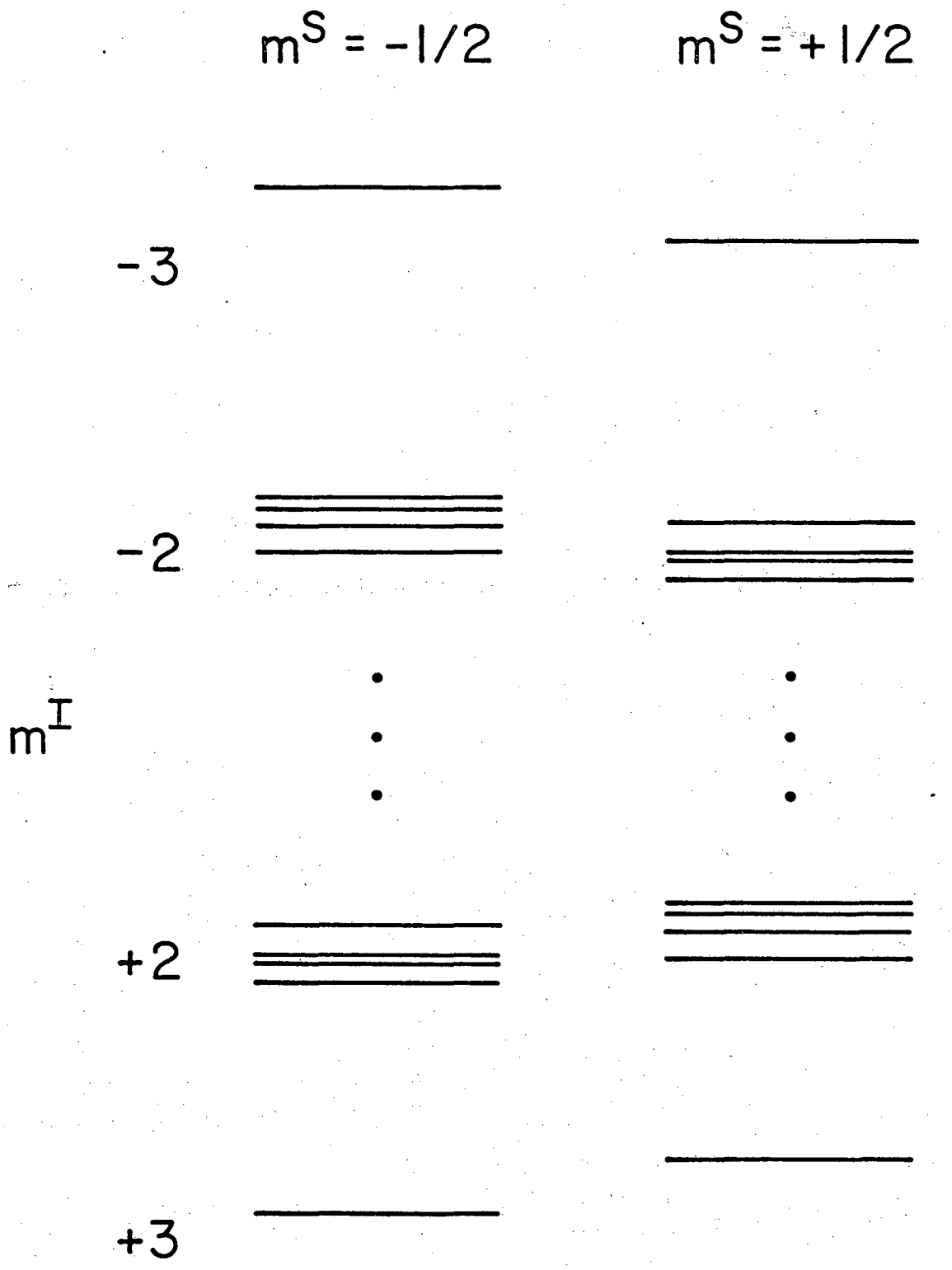

Figure 6

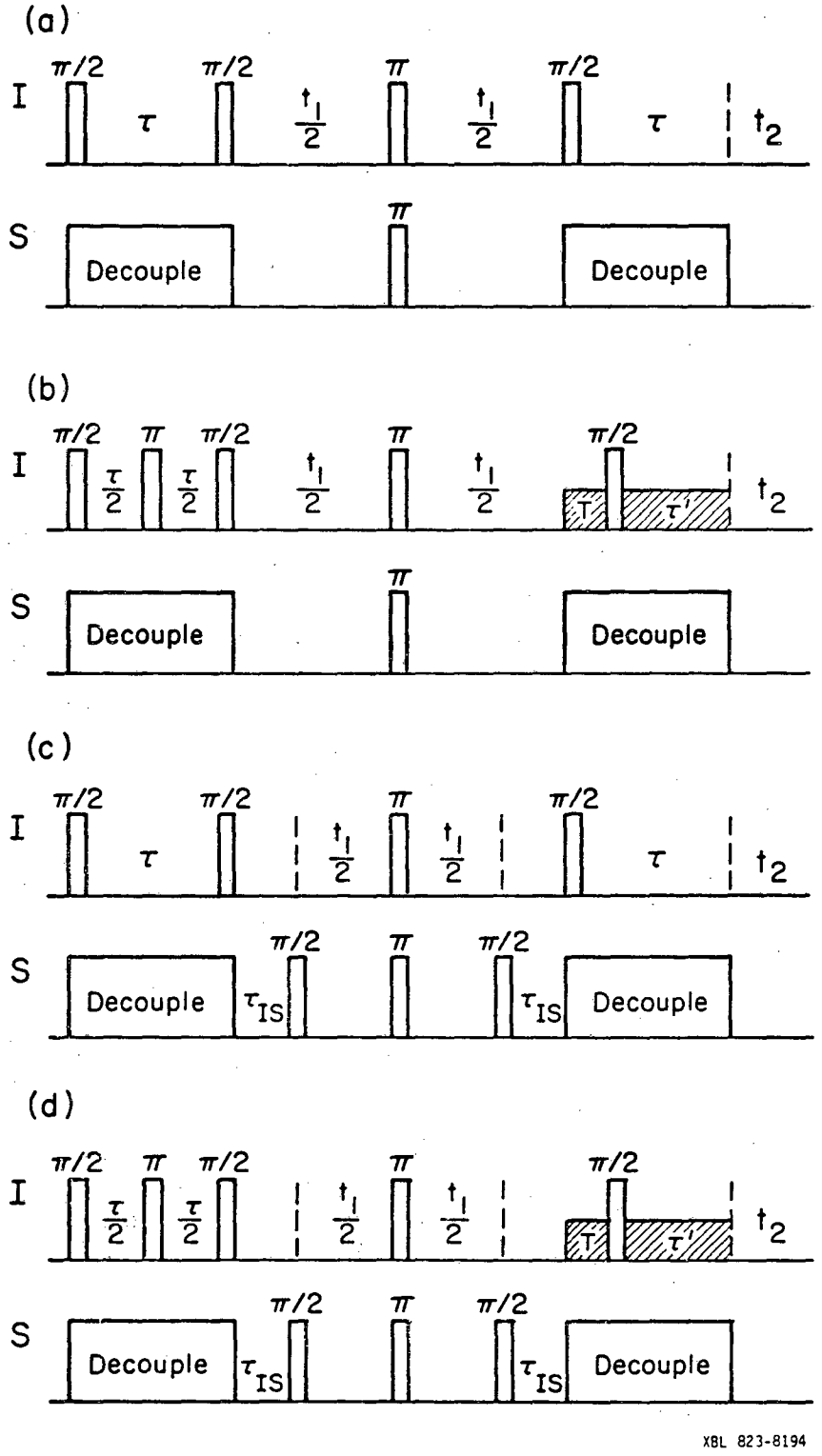
(a)
I
π/2
τ
π/2
t1/2
π
t1/2
π/2
τ
t2
S
Decouple
π
Decouple
(b)
I
π/2
τ/2
π
τ/2
π/2
t1/2
π
t1/2
π/2
T
τ'
t2
S
Decouple
π
Decouple
(c)
I
π/2
τ
π/2
t1/2
π
t1/2
π/2
τ
t2
S
Decouple
π/2
τIS
π
π/2
τIS
Decouple
(d)
I
π/2
τ/2
π
τ/2
π/2
t1/2
π
t1/2
π/2
T
τ'
t2
S
Decouple
π/2
τIS
π
π/2
τIS
Decouple
XBL 823-8194

Figure 7

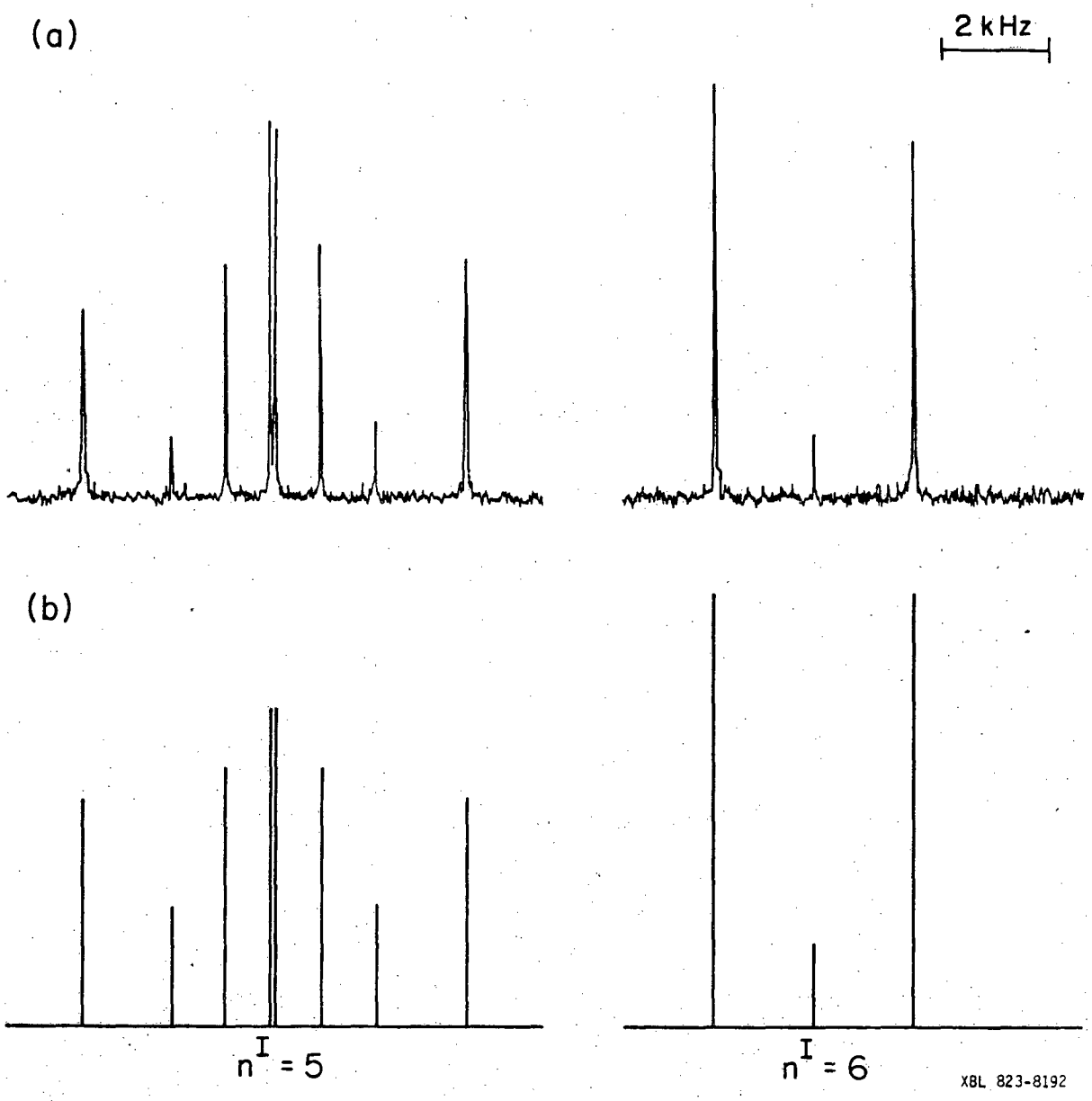

Figure 8

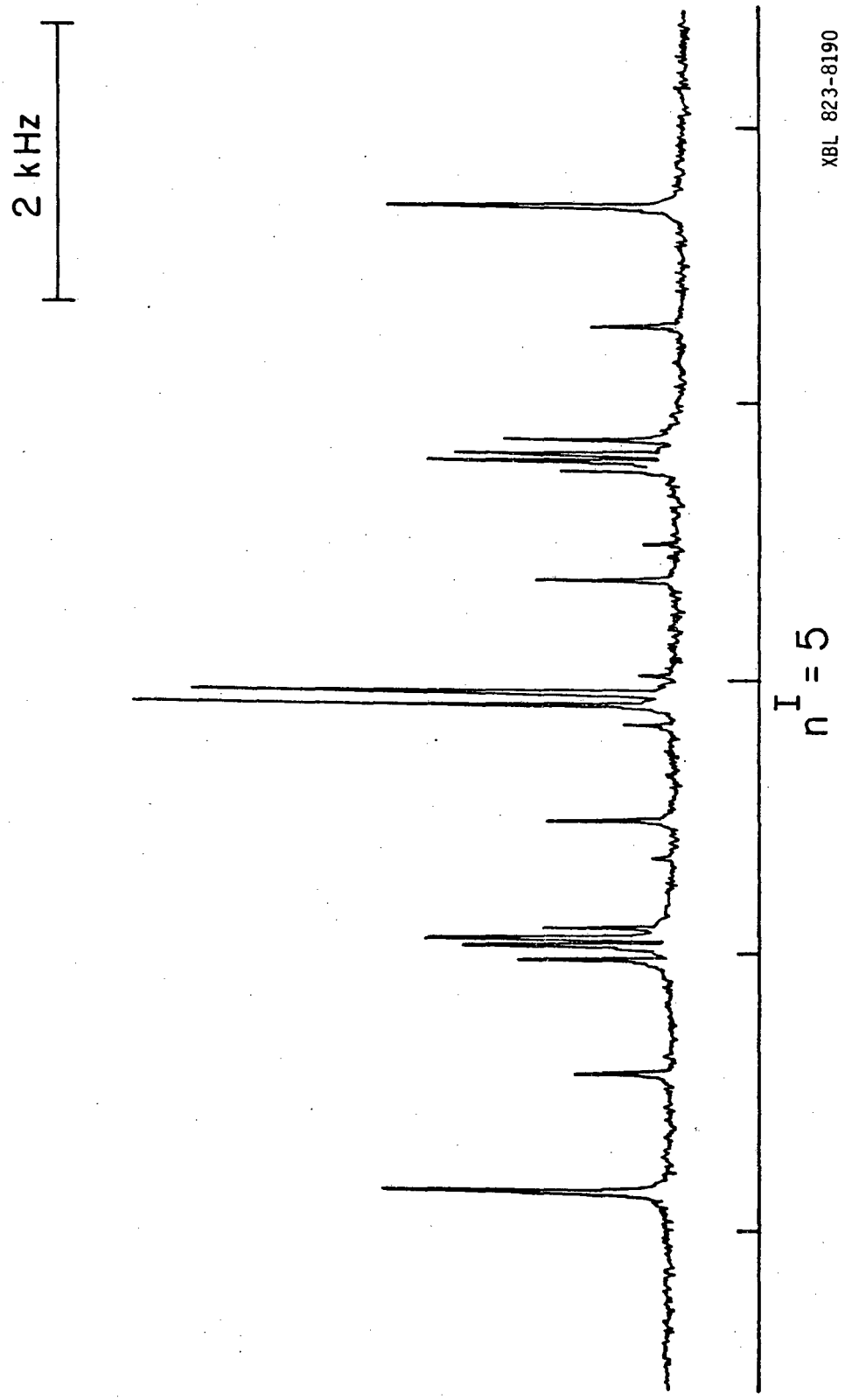

Figure 9

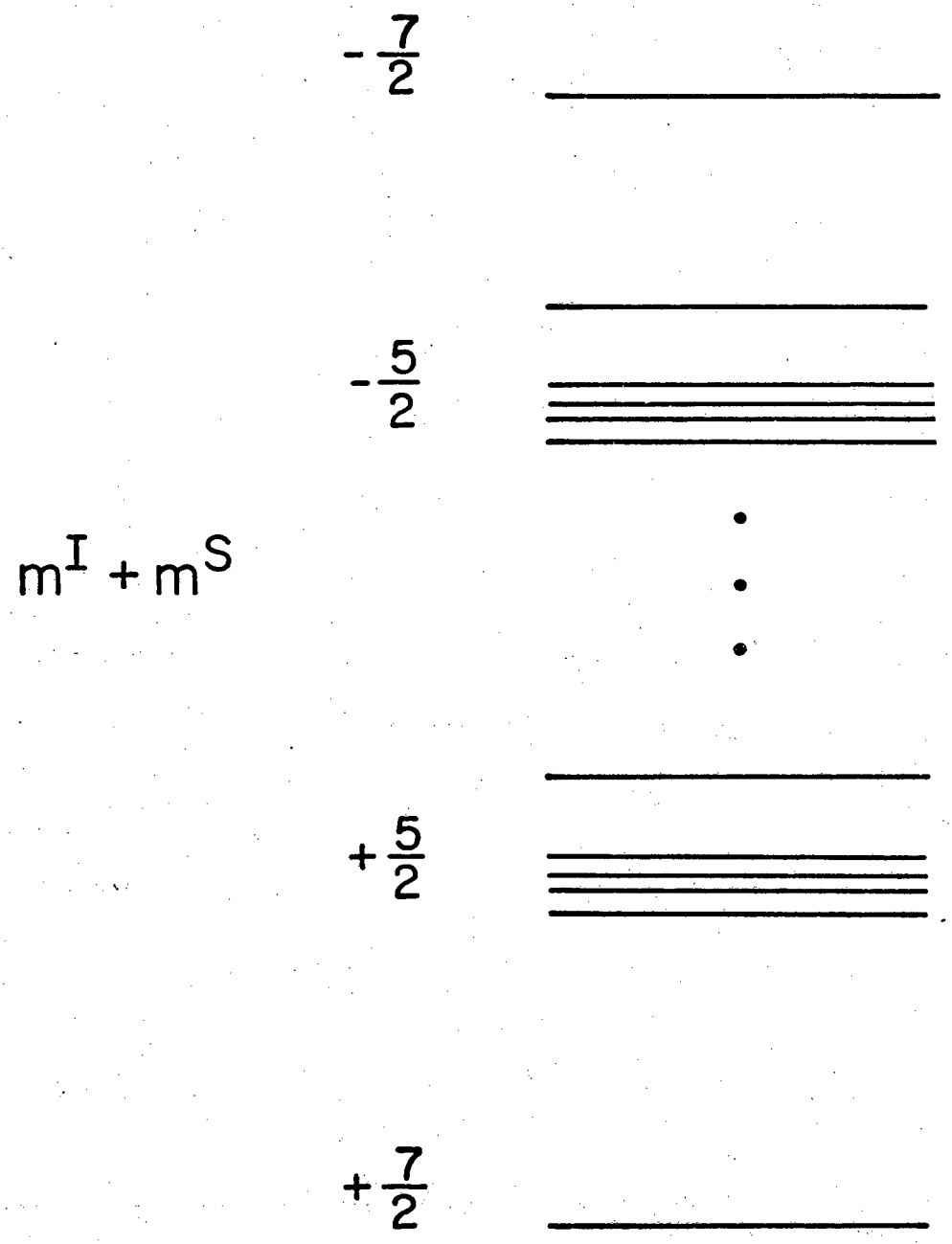

Figure 10

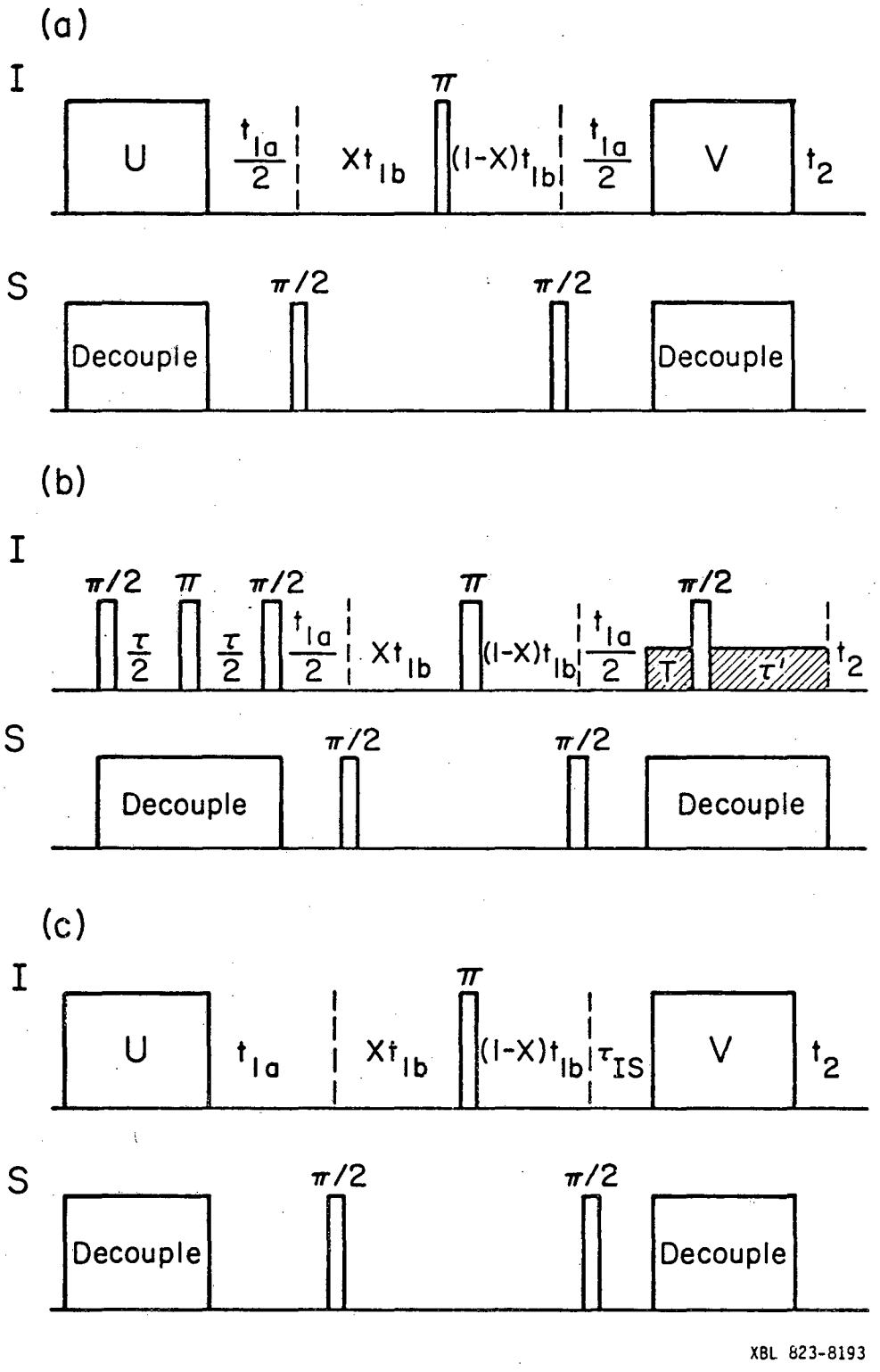
(a)
I
U
$\frac{t_{1a}}{2}$
Xt_{1b}
π
$(1-X)t_{1b}$
$\frac{t_{1a}}{2}$
V
t_2
S
Decouple
π/2
π/2
Decouple
(b)
I
π/2
$\frac{\tau}{2}$
π
$\frac{\tau}{2}$
π/2
$\frac{t_{1a}}{2}$
Xt_{1b}
π
$(1-X)t_{1b}$
$\frac{t_{1a}}{2}$
π/2
τ
τ'
t_2
S
Decouple
π/2
π/2
Decouple
(c)
I
U
t_{1a}
Xt_{1b}
π
$(1-X)t_{1b}$
τ_{IS}
V
t_2
S
Decouple
π/2
π/2
Decouple
XBL 823-8193

Figure 11

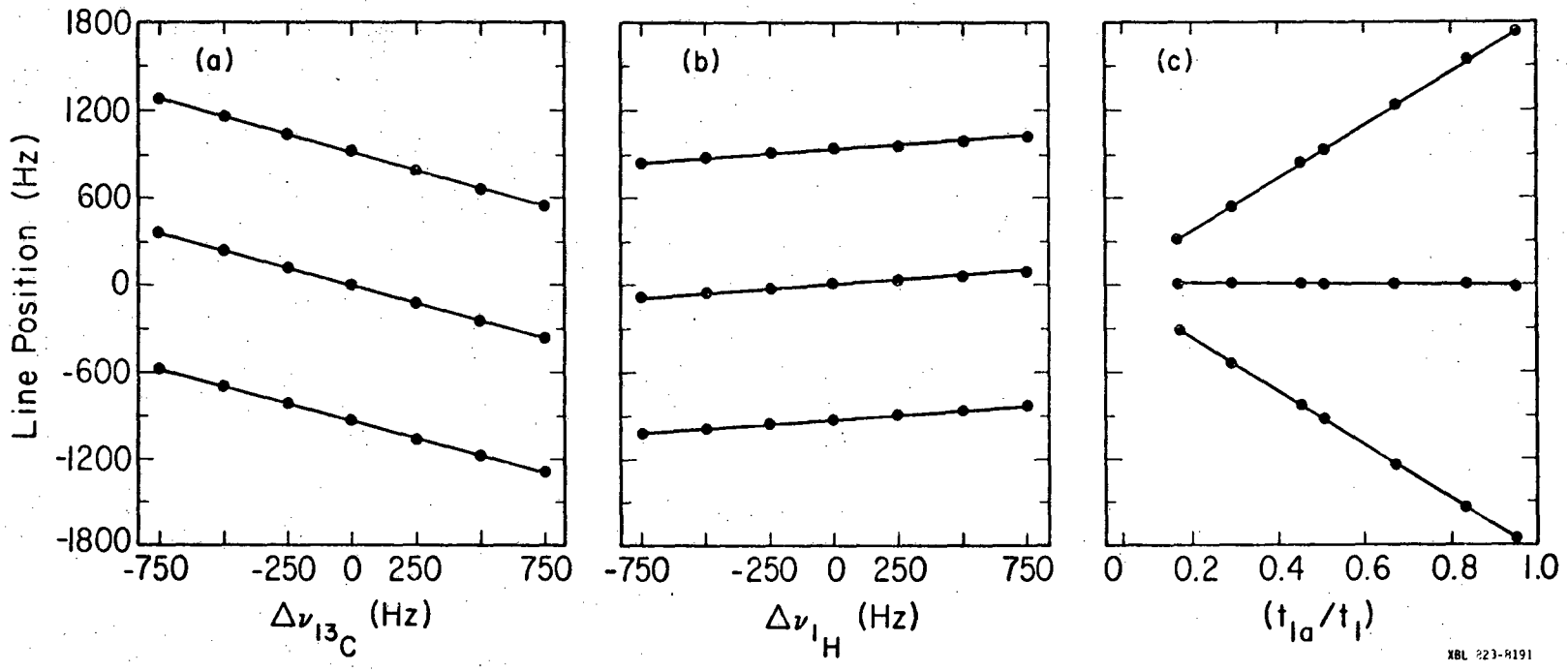
(a)
(b)
(c)
Line Position (Hz)
1800
1200
600
0
-600
-1200
-1800
-750
-250
0
250
750
$\Delta\nu_{^{13}C}$ (Hz)
$\Delta\nu_{^{1}H}$ (Hz)
0
0.2
0.4
0.6
0.8
1.0
(t_{1a}/t_1)
XBL 823-8191

Figure 12

This report was done with support from the Department of Energy. Any conclusions or opinions expressed in this report represent solely those of the author(s) and not necessarily those of The Regents of the University of California, the Lawrence Berkeley Laboratory or the Department of Energy.

Reference to a company or product name does not imply approval or recommendation of the product by the University of California or the U.S. Department of Energy to the exclusion of others that may be suitable.

TECHNICAL INFORMATION DEPARTMENT
LAWRENCE BERKELEY LABORATORY
UNIVERSITY OF CALIFORNIA
BERKELEY, CALIFORNIA 94720